

1 **Xylem and phloem in petioles are coordinated with leaf gas exchange in oaks with**  
2 **contrasting anatomical strategies depending on leaf habit**

3 Rubén Martín-Sánchez\*<sup>1</sup>, Domingo Sancho-Knapik<sup>1,2</sup>, Juan Pedro Ferrio<sup>3</sup>, David Alonso-Forn<sup>4</sup>, Juan  
4 Manuel Losada<sup>5</sup>, José Javier Peguero-Pina<sup>1,2</sup>, Maurizio Mencuccini<sup>6,7</sup>, Eustaquio Gil-Pelegrín<sup>3</sup>

6 <sup>1</sup>Departamento de Sistemas Agrícolas, Forestales y Medio Ambiente, Centro de Investigación y  
7 Tecnología Agroalimentaria de Aragón (CITA), Avda. Montañana 930, 50059, Zaragoza, Spain

8 <sup>2</sup>Instituto Agroalimentario de Aragón -IA2- (CITA-Universidad de Zaragoza), Zaragoza, Spain

9 <sup>3</sup>Estación Experimental de Aula Dei, Consejo Superior de Investigaciones Científicas (EEAD-CSIC),  
10 Avda. Montañana 1005, Zaragoza 50059, Spain

11 <sup>4</sup>Research Group on Plant Biology Under Mediterranean Conditions, Department of Biology, University  
12 of Balearic Islands (UIB). Ctra Valldemossa km 7,5 E-07122 Palma, Balearic Islands, Spain.

13 <sup>5</sup>Institute for Mediterranean and Subtropical Horticulture -La Mayora- (IHSM La Mayora—CSIC—  
14 UMA), Avda. Dr. Wienberg s/n, 29750 Malaga, Spain

15 <sup>6</sup>CREAF, Campus UAB, Cerdanyola del Vallés, Spain

16 <sup>7</sup>ICREA, Barcelona, Spain

17  
18 \* Corresponding author: Rubén Martín-Sánchez

19  
20 **Email addresses** of all the authors

21 RMS: [rmartin@cita-aragon.es](mailto:rmartin@cita-aragon.es)

22 DSK: [dsancho@cita-aragon.es](mailto:dsancho@cita-aragon.es)

23 JPF: [jpferrio@eead.csic.es](mailto:jpferrio@eead.csic.es)

24 DAF: [david.alonso@uib.es](mailto:david.alonso@uib.es)

25 JML: [juan.losada@csic.es](mailto:juan.losada@csic.es)

26 JJPP: [jjpeguero@cita-aragon.es](mailto:jjpeguero@cita-aragon.es)

27 MM: [m.mencuccini@creaf.uab.cat](mailto:m.mencuccini@creaf.uab.cat)

28 EGP: [gilpelegrin@eead.csic.es](mailto:gilpelegrin@eead.csic.es)

29  
30 **ORCID identifier** of authors (for non-ambiguous identification of authors)

31  
32 Rubén Martín-Sánchez: 0000-0002-0288-3869

33 Domingo Sancho-Knapik: 0000-0001-9584-7471

34 Juan Pedro Ferrio: 0000-0001-5904-7821

35 David Alonso-Forn: 0000-0002-1467-1943

36 Juan Manuel Losada: 0000-0002-7966-5018

37 Jose Javier Peguero-Pina: 0000-0002-8903-2935

38 Maurizio Mencuccini: 0000-0003-0840-1477

39 Eustaquio Gil-Pelegrín: 0000-0002-4053-6681

40  
41 **Keywords:** Conductive tissues, hydraulic conductivity, petioles, *Quercus*, leaf habit,  
42 stomatal conductance, photosynthesis

43

44 ABSTRACT

45 As the single link between leaves and the rest of the plant, petioles must develop  
46 conductive tissues according to the water influx and sugar outflow of the leaf lamina. A  
47 scaling relationship between leaf area and anatomical traits of xylem and phloem is  
48 expected to improve the efficiency of these tissues. However, the different constraints  
49 compromising the functionality of both tissues (e.g., risk of cavitation) must not be  
50 disregarded. Additionally, plants present two main leaf habits (deciduous and evergreen)  
51 that may have different strategies to produce and package their petiole conduits to cope  
52 with environmental restrictions. In this study, we explore, in a diverse group of 33 oak  
53 species, the relationships between petiole anatomical traits, leaf area, stomatal  
54 conductance and photosynthesis rate. Results showed allometric scaling between  
55 anatomical structure of xylem and phloem with leaf area. We also found how  
56 photosynthesis and stomatal conductance at leaf-level are correlated with anatomical  
57 traits in the petiole. Nonetheless, the main novelty is how oaks present a different strategy  
58 depending on the leaf habit. Deciduous species tend to increase their diameters to achieve  
59 a greater leaf-specific conductivity. By contrast, evergreen oaks develop larger xylem  
60 conductive areas for a given leaf area than deciduous ones. This trade-off between safety-  
61 efficiency in petioles has never been attributed to the leaf habit of the species.

62

63 INTRODUCTION

64 Petioles, besides accomplishing a structural function, link the main photosynthetic organs  
65 —i.e., leaf laminae— with the rest of the plant. In this regard, they may act as a bottleneck  
66 in the soil-plant-atmosphere continuum for water transport and the translocation of  
67 photosynthates (Brocious and Hacke, 2016). Thus, transpiration has been traditionally  
68 related to transport capacity of xylem and photosynthesis rate to export capacity of  
69 phloem in petioles (Salisbury, 1913; Brocious and Hacke, 2016). However, this  
70 correlation has been questioned within angiosperms (Gleason et al., 2016). These authors  
71 reported a weak or even absent coordination between hydraulic capacity and gas  
72 exchange capacity.

73 Petioles must contain enough xylem vessels and sieve tubes to, respectively, supply water  
74 to the leaf lamina and export assimilates from the leaf to the rest of the plant. For this  
75 reason, a scaling relationship between leaf area and both xylem and phloem structures  
76 (area of conductive tissues and size of the conduits) in petioles is expected (Ray and  
77 Jones, 2018). The number and size of the conduits ultimately reflects the transport ability  
78 —namely, the hydraulic conductivity ( $K_h$ )— of the conductive tissues according to the  
79 Hagen-Poiseuille law (Tyree and Zimmermann, 2002; Hirose et al., 2005; Woodruff,  
80 2014). Nonetheless, the  $K_h$  only shows how much fluid is potentially able to be moved  
81 along a pathway whereas two petioles with the same  $K_h$  can support different leaf areas.  
82 For this reason, the leaf-specific conductivity (LSC) of a petiole provides a more  
83 physiological explanation of a leaf's efficiency as LSC is the capacity to supply water ( $K_h$ )  
84 per leaf area. LSC can also be expressed as the product of the specific conductivity ( $K_s$ ,  
85 i.e.  $K_h$  per conductive area ratio) and the Huber value ( $H_v$ , i.e. conductive area per leaf  
86 area ratio) (Mencuccini et al., 2019). Therefore, the same LSC can be achieved in different  
87 ways by modulating both  $K_s$  and  $H_v$ . Indeed, Mencuccini et al. (2019) found in a wide  
88 range of plant species a negative relationship between  $K_s$  and  $H_v$  in stems. What are the  
89 implications of increasing each variable?

90 Increasing the Huber value, that is, allocating more cross-sectional area to a conductive  
91 function, would imply a reduction in the availability of space for structural support. This  
92 could result in a possible trade-off between both kind of tissues (Zwieniecki et al., 2004).  
93 By contrast, as the specific conductivity mainly depends on the diameter of the conduits,  
94 the hydraulic capacity of the petiole is compromised by the same factors that determine  
95 its vulnerability, as in any other parts of the plant (Hacke and Sauter, 1996) In fact, it has

96 been suggested that petioles may act as hydraulic fuses for the plant through higher  
97 vulnerability to embolism than stems, thereby ensuring resilience to extreme drought  
98 events (Peguero-Pina et al., 2015; Alonso-Forn et al., 2021). Throughout their lifespan,  
99 leaves can be affected by climatic stresses (e.g. aridity or cold) that may influence the size  
100 of the xylem conduits (Gil-Pelegrín et al., 2017). In this sense, many studies showed a  
101 higher vulnerability to cavitation in species with wider vessels (Hacke et al., 2000; Tyree,  
102 2003; Hacke et al., 2006; Cai and Tyree, 2010; Jacobsen et al., 2019; Blackman et al.,  
103 2023). Embolized xylem conduits leads to hydraulic failure, which is the main cause of  
104 plant mortality in response to drought (Tyree and Sperry, 1989). By contrast, many species  
105 inhabiting very stressful habitats reduce the diameter of their conduits, achieving a higher  
106 resistance to cavitation. This reduction in the conduit diameter results in a lower water  
107 transport efficiency (Giordano et al., 1978). However, this decrease may be compensated  
108 by increasing the number of conduits (Nardini et al., 2012). When cavitation is caused by  
109 freeze-thaw cycles, the same arguments arise. Wider conduits are likewise more  
110 vulnerable than small ones because they contain greater dissolved air which can form  
111 larger bubbles causing cavitation at lower tensions (Cochard and Tyree, 1990; Sperry and  
112 Sullivan, 1992; Lo Gullo and Salleo, 1993; Lemoine et al., 1999; Sevanto, et al., 2012;  
113 Zanne et al., 2014; Ni et al., 2022).

114 Regarding the phloem, other factors rather than climatic stresses might influence the size  
115 of its conduits. Sugars, amino acids and other organic metabolites in the sap make sieve  
116 tubes a target for some phytophagous insects like aphids (Will et al., 2013). When an  
117 aphid stings a sieve tube with its stylet, the plant responds by occluding the sieve plates  
118 with callose, turning it into a non-functional conduit (Will and van Bel, 2006). Thus,  
119 building more but smaller sieve elements is safer than building a few large conduits  
120 (Ewers and Fisher, 1991). Besides, wider sieve elements would need to load more sugars  
121 in the source (i.e., the leaf), to generate enough turgor pressure gradient for sap to flow  
122 towards the sink organs (Hölttä et al., 2009; Sevanto, 2014).

123 The scaling relationship between xylem and phloem areas has been explored in several  
124 species (Jyske and Hölttä, 2015; Carvalho et al., 2017a; Carvalho et al., 2017b;  
125 Kiorapostolou and Petit, 2018; Ray and Jones, 2018; Losada et al., 2022). Most of the  
126 studies focus on stems, although Ray and Jones (2018) analyzed petioles in several  
127 *Pelargonium* species. Albeit plants tend to present more xylem than phloem, an  
128 isometrical scaling has been found in these studies. Nonetheless, most research focuses

129 on a single species. To our knowledge, they do not conduct comparative analyses across  
130 different leaf longevities, even in genus level studies. Deciduousness and evergreenness  
131 offer different solutions to cope with climatic stresses, which are, in turn, closely related  
132 to specific leaf area (SLA) (Sancho-Knapik et al., 2021) (Fig. 1). Similarly, these climatic  
133 stresses have been demonstrated to limit the growth of the conduits, even in petioles  
134 (Blackman et al., 2023). Since the LSC ultimately depends on the leaf area, the Huber  
135 value and the diameter of the conduits, we wonder if the two different leaf habits could  
136 develop two different strategies (Fig. 1, models A and B) to reach similar values of LSC.

137 The genus *Quercus* (oaks) offers an excellent system to study the scaling between both  
138 conductive tissues, xylem and phloem, besides its ecophysiological implications. Oaks  
139 represent a single monophyletic clade with over 400 species occupying very different  
140 habitats around the northern hemisphere, from tropical rainforests to cold temperate  
141 forests through semideserts and chaparrals. Additionally, oak species exhibit a much  
142 broader range not only in terms of leaf area, but also in leaf lifespan compared to other  
143 widely studied genera such as *Populus*, *Pelargonium* or *Eucalyptus* (Brocius and Hacke,  
144 2016; Ray and Jones, 2018; Blackman et al., 2023). The variability in leaf area can  
145 suppose a difference of 70 times between the species with the largest and the smallest  
146 leaves (Sancho-Knapik et al., 2021). Finally, phenology ranges from deciduous with a  
147 lifespan of just five months up to evergreen species whose leaves can persist over several  
148 years (Mediavilla et al., 2008; Harayama et al., 2016).

149 In this study we explore the scaling relationships among the different xylem and phloem  
150 traits in petiole cross-sections, leaf area, stomatal conductance, photosynthesis rate and  
151 climatic variables in 33 oak species (16 deciduous and 17 evergreen) covering the full  
152 range of variation in oaks in terms of leaf area and leaf habit. Based on the information  
153 presented thus far (Fig. 1), four aims were addressed: 1) to explore the scaling  
154 relationships between conductive tissue structures in petioles —i.e., conductive area and  
155 hydraulic diameter of the conduits— and leaf area, for both xylem and phloem; 2) to  
156 verify whether deciduous and evergreen species exhibit the same LSC, and to check if  
157 deciduous and evergreen oaks follow a different strategy when producing and packaging  
158 their conduits to improve their efficiency; 3) in case that two different models are  
159 observed, to relate them with climatic variables (mainly aridity and cold) that could be  
160 explaining such differences; 4) to assess if the hydraulic architecture resulting from the  
161 observed scaling correlates with the physiological demands of the leaf, i.e., stomatal

162 conductance and photosynthesis rate. We hypothesized that xylem and phloem petiole  
163 traits should scale proportionally with leaf area, which ultimately reflects the water  
164 demands (stomatal conductance) and export requirements (photosynthesis rate) of the leaf  
165 lamina.

166

## 167 MATERIAL AND METHODS

### 168 *Plant material*

169 In this study, we sampled 22 oak species occurring in the living collection in CITA de  
170 Aragón (41°39'N, 0°52'W, 200 m a.s.l., Zaragoza, Spain). In order to get a greater  
171 diversity of species and to cover a wider range of leaf areas, we also sampled 11 additional  
172 species from Jardín Botánico de Iturrarán 43°15'N 2°09.3'W, 200 m a.s.l., Gipuzkoa,  
173 Spain).

174 We sampled five mature leaves of south-exposed branches from 3-5 trees per species.  
175 They were sealed in plastic bags and carried to the laboratory. The mid-section of the  
176 petiole was cut and stored in 70% ethanol. Then, leaf area (LA) was measured using  
177 ImageJ software by scanning the leaf lamina.

178

### 179 *Anatomical traits*

180 Petiole sections were dehydrated in a graded ethanol series and subsequently embedded  
181 in Paraplast Plus embedding medium (Leica, Richmond, IL, USA). The resulting paraffin  
182 blocks were cut in the microtome (HM 350S; MICROM, Walldorf, Germany) to obtain  
183 15-20  $\mu\text{m}$  cross-sections that were stained with saffranine (0.1% w/v), picric acid (0.5%  
184 v/v) and AstraBlue (0.1% w/v) after being deparaffinated with Isoparaffin H and  
185 rehydrated using a graded ethanol series (100, 95, 90 and 70 %). Then, sections were  
186 observed and photographed under a light microscope (OPTIKA B-600TiFL; Optika  
187 Microscopes, Ponteranica, Italy) (Fig. 2). We measured the total petiole cross-sectional  
188 area ( $A_{pet}$ ), as well as the conductive area, i.e., the sum of xylem and phloem areas (Fig.  
189 2a). Hereafter, we will use conductive area ( $A_c$ ) to refer to the sum of the two vascular  
190 tissues and we will distinguish between xylem area ( $A_x$ ) and phloem area ( $A_p$ ) when  
191 treated separately. Besides, we measured the total number of xylem vessel elements and  
192 phloem conduits and their mean diameter in three subsamples of the whole conductive

193 area of each tissue per photograph (Fig. 2b, 2c). In the phloem, our aim was to measure  
194 only sieve tubes; however, we cannot claim to have exclusively measured these ones since  
195 a visible sieve tube plate (or their identification with callose staining) is necessary to  
196 properly identify a sieve tube. We discarded the first brick-shaped cell layers (i.e., the  
197 procambium). Medullary rays and cells with a visible nucleus and organelles were also  
198 neglected. Finally, very small cells (what we interpret as companion cells or oblique/bevel  
199 cuts) as well as the big rounded thick-wall cells in the distal part of the phloem (phloem  
200 fibers) were also avoided (Esau, 1939). The rest of the cells were considered as potentially  
201 sieve tubes and as such, measured. Afterwards, we calculated the hydraulic diameter for  
202 xylem ( $d_{hx}$ ) and phloem ( $d_{hp}$ ) using the formula proposed by Sperry et al. (1994):

$$203 \quad d_h = \frac{\sum_i d_i^5}{\sum_i d_i^4}$$

204 where  $d_i$  is the mean diameter of each conduit measured. Then, we also calculated the  
205 ratio of the conductive area normalized by the leaf area following the next formula:

$$206 \quad \text{For xylem: } XLA = \frac{A_x}{LA \times 10000} \quad ; \quad \text{For phloem: } PLA = \frac{A_p}{LA \times 10000}$$

207

208 Where  $A_x$  is the total xylem area,  $A_p$  is the total phloem area and LA is leaf area. Leaf area  
209 was multiplied by 10 000 to obtain values close to one and to transform units to  $\text{cm}^2 \text{m}^{-2}$ .  
210 All measurements were done using ImageJ software. Traits analyzed are compiled in  
211 Table 1.

212

### 213 *Hydraulic conductivity*

214 We calculated the theoretical hydraulic conductivity of the whole petiole ( $K_h$ ) as the sum  
215 of each conduit conductivity assuming that both types, xylem vessels ( $K_{hx}$ ) and phloem  
216 cells ( $K_{hp}$ ), follow the Hagen-Poiseuille law (Tyree and Zimmermann, 2002; Hirose et al.,  
217 2005; Woodruff, 2014):

$$218 \quad K_h = \sum_i \frac{d_i^4 \pi \rho}{128 \eta}$$

219 where  $\rho$  is the density of the fluid moving along the conduits at 25 °C, assuming pure  
220 water for xylem (997kg m<sup>-3</sup>) and a specific sap density dependent of sucrose concentration  
221 for phloem (1068 kg m<sup>-3</sup>) (Jensen et al., 2013),  $\eta$  is the viscosity of the fluid at 25 °C, pure  
222 water for xylem (8.9 x 10<sup>-10</sup> MPa s) and 1.91 times that value for phloem sap (1.7 x 10<sup>-9</sup>  
223 MPa s) (Thomson, 2006; Jensen et al., 2013); and  $d_i$  is the mean lumen diameter of each  
224 conduit.

225 Additionally, we calculated leaf-specific hydraulic conductivity of xylem (LSC):

$$226 \quad LSC = \frac{K_{hx}}{LA}$$

227 where LA is leaf area. We also calculated the specific conductivity for xylem ( $K_{sx}$ ):

$$228 \quad K_{sx} = \frac{K_{hx}}{A_x}$$

229 where  $A_x$  is the area of xylem in the cross-section of the petiole.

230

### 231 *Climatic variables*

232 To get a mean representative value of different climatic variables for each species we  
233 followed the same procedure as in Martín-Sánchez et al. (2024). In short, we first  
234 downloaded GBIF individual presence points for the 33 species studied, we thinned the  
235 data to one presence point per square kilometer using SDMtune R package (Vignali et al.,  
236 2020) and we extracted the climatic variables from the WorldClim version 2.1 database  
237 (Fick and Hijmans, 2017. WorldClim 2. <https://www.worldclim.org>). We additionally  
238 added an aridity index (AI) calculated as mean annual precipitation (MAP) divided by  
239 potential evapotranspiration (PET) (Mencuccini et al., 2019; Peguero-Pina et al., 2020).  
240 All individual values were summarized into a mean value for each species. To test our  
241 hypothesis whether hydraulic diameters are restrained by climatic factors, we chose  
242 variables related to cold and aridity: mean annual temperature (MAT), mean of daily  
243 minimum temperatures during the coldest quarter ( $T_{min}$ ), mean annual precipitation  
244 (MAP) and the aridity index (AI).

245

### 246 *Leaf gas exchange*



247 We obtained the mean photosynthesis rate ( $A_N$ ) and stomatal conductance ( $g_s$ ) of 26  
248 species. For nine species, we measured these parameters using an open gas exchange  
249 system (CIRAS-3, PP-Systems, Amesbury, MA, USA) fitted with an automatic universal  
250 leaf cuvette (PLC6-U, PP-Systems, Amesbury, MA, USA) in six leaves per species from  
251 our living collection. All measurements were conducted under the following standard  
252 environmental conditions: CO<sub>2</sub> concentration surrounding the leaf ( $C_a$ ) of 400  $\mu\text{mol mol}^{-1}$ ,  
253 leaf temperature of 25 °C, vapor pressure deficit of 1.25 kPa and saturating  
254 photosynthetic photon flux density of 1500  $\mu\text{mol m}^{-2} \text{s}^{-1}$ . We complemented our own  
255 measurements with data for 17 species compiled from other studies (Vaitkus and McLeod,  
256 1995; Nagel et al., 2002; Thadani et al., 2009; Huang et al., 2016; Llusia et al., 2016;  
257 Jafarnia et al., 2018; Alonso-Forn et al., 2020; Kar et al., 2021). Assuming a mean value  
258 of  $A_N$  and  $g_s$  for each species and taking into account the mean LA measured for each  
259 species, we calculated the theoretical mean photosynthesis rate and stomatal conductance  
260 at whole leaf level. ( $A_{N,leaf}$  and  $g_{s,leaf}$ , respectively).

261

#### 262 *Statistical analyses*

263 First, we tested the potential effect of the garden throughout several analyses of variance  
264 (ANOVAs) and linear regressions via mixed models. On the one hand, we performed  
265 ANOVAs for each single trait to see how much variance was explained by species and  
266 the garden (Table S1). On the other hand, we did linear regressions via mixed models  
267 including the garden as a random factor in correlations between pairwise traits, besides a  
268 subsequent ANOVA to see how much variance is explained by the random factor.  
269 Variance explained by garden in the first ANOVA showed that, for every trait, species  
270 accounted for more variance than the garden and in most of the cases species accounted  
271 over 60% of variance. Besides, correlations remain significant even when garden is  
272 included as a random factor (Table S2). Finally, when we tested differences in the leaf  
273 habit, we additionally accounted for garden and the interaction between leaf habit and  
274 garden in the ANOVAs. In most of the cases, the interaction resulted to be non-significant,  
275 except for three traits (Table S3). Even among those exceptions leaf habit and/or residuals  
276 accounted for more variance than the garden. In view of these results, we conclude that  
277 correlations are not strongly skewed by an effect of the garden.

278 Cross-correlations were performed between the different anatomical, hydraulic and  
279 physiological traits, assuming a log-log correlation. Alternatively, linear cross-  
280 correlations were performed between xylem and phloem hydraulic diameters and climatic  
281 variables. Post-hoc analyses of every regression fit were performed using DHARMA R  
282 package to test normality, homoscedasticity and outliers (Hartig, 2022). Additionally, we  
283 used SMATR R package to check if the scaling relationships were isometric or allometric  
284 (Warton et al., 2012). This calculates the slope for the bivariate linear relationship  
285 between two variables (after being  $\log_{10}$ -transformed) following the standardized major  
286 axis regression. If the 95% confidence interval of the slope includes the value of 1,  
287 isometry cannot be rejected, whereas allometry can be assumed when this confidence  
288 interval does not include such value. For anatomical traits and conductivities, we  
289 performed slope tests including leaf habit as factor. Finally, for physiological traits, all  
290 species were considered together.

291

## 292 RESULTS

293 The range of variation covered in this study in terms of leaf area goes from 1.9 cm<sup>2</sup>  
294 (*Quercus monimotricha*) up to 151 cm<sup>2</sup> (*Quercus macrocarpa*). If species are compared  
295 by their leaf habit, significant differences ( $P < 0.001$ ) can be found between deciduous  
296 (DEC;  $68.7 \pm 46$  cm<sup>2</sup>) and evergreen (EVE;  $16.6 \pm 15$  cm<sup>2</sup>) (Fig. 3a). Raw measurements  
297 of all the measured diameters are represented as a violin plot to notice the range of  
298 variation either between leaf habits or between conductive tissues (Fig. 3b). Hydraulic  
299 diameter ( $d_h$ ) is always significantly wider — either for xylem ( $d_{hx}$ ) or phloem ( $d_{hp}$ ) — in  
300 deciduous than in evergreen species although the range of variation in xylem vessels  
301 diameter ( $25 \pm 7.64$   $\mu$ m in deciduous;  $15.8 \pm 5.6$   $\mu$ m in evergreen) is higher than in phloem  
302 cells diameter ( $8.19 \pm 1.77$   $\mu$ m in deciduous;  $6.28 \pm 1.42$   $\mu$ m in evergreen). When the  
303 conductive area ( $A_c$ ) is examined (Fig. 3c), deciduous species also display larger xylem  
304 and phloem cross-sectional areas ( $A_x = 297 \pm 180 \times 10^3$   $\mu$ m<sup>2</sup>,  $A_p = 224 \pm 147 \times 10^3$   $\mu$ m<sup>2</sup>)  
305 compared to evergreen species ( $A_x = 175 \pm 121 \times 10^3$   $\mu$ m<sup>2</sup>,  $A_p = 128 \pm 116 \times 10^3$   $\mu$ m<sup>2</sup>)  
306 (Fig. 2c). Nonetheless, the ratio between cross-sectional areas of the vascular elements in  
307 the petiole and LA —i.e., XLA and PLA —, reveals significantly lower values in  
308 deciduous species (XLA =  $4628 \pm 1371$ , PLA =  $3885 \pm 2320$ ) compared with evergreen  
309 species (XLA =  $14207 \pm 9038$ , PLA =  $9242 \pm 3923$ ) (Fig. 3d), which means that evergreen  
310 oaks have a higher conductive area per leaf area. Calculated xylem hydraulic conductivity

311 ( $K_{hx}$ ) and xylem specific conductivity ( $K_{sx}$ ) also present highly significant ( $P < 0.001$ )  
312 differences between deciduous and evergreen species. By contrast,  $K_{hp}$  does not show  
313 significant differences when leaf habit is considered ( $P = 0.902$ ) (Table 2).

314 Although the cross-sectional petiole ( $A_{pet}$ ) area shows a positively significant relationship  
315 with LA ( $P < 0.001$ ), the dispersion of the data is quite high, especially in deciduous  
316 species (DEC:  $R^2 = 0.486$ , EVE  $R^2 = 0.752$ ) (Fig. 4a). Conductive area ( $A_c$ ) presents a  
317 strong correlation with LA for both leaf habits ( $P < 0.001$ , DEC:  $R^2 = 0.816$ , EVE  $R^2 =$   
318  $0.816$ ) (Fig. 4b, Table 3).

319

### 320 *Xylem and phloem anatomy*

321 We analyze how the conductive area of both tissues, xylem and phloem, as well as the  
322 hydraulic diameter of conduits scale with leaf area. In all cases, traits scale positively and  
323 significantly ( $P < 0.001$ ) with LA (Fig. 5, Table 3). The larger a leaf is, the larger is the  
324 investment in conductive area (Fig. 5a, d) and wider conduits (Fig. 5b, e). However, the  
325 relationships are not linear but logarithmic, so that for small leaves, a slight increment in  
326 leaf area implies a big increase in both,  $A_c$  and  $d_h$ , especially in evergreen species. Xylem  
327 and phloem also present the same behavior when their ratios are analyzed, i.e., how much  
328  $A_x$  and  $A_p$  a petiole develops divided by leaf area (Fig. 5c, f). XLA and PLA scale  
329 negatively and significantly ( $P < 0.001$ ) with LA either for deciduous or evergreen species  
330 (Fig. 5c, f). Evergreen species show a huge heterogeneity in their ratio values for both  
331 xylem and phloem for the smallest values of LA. In other words, there is a group of small-  
332 leaved evergreen species that invests more in  $A_x$  for a specific LA in comparison to large-  
333 leaved evergreen leaves. XLA and PLA values above a LA of c.a.  $50 \text{ cm}^2$  become  
334 asymptotical. The scaling relationships are allometric in all cases (Table 3).

335 When both conductive areas are correlated, a strong linear relationship ( $P < 0.001$ ) can be  
336 appreciated (Fig. S1;  $R^2 = 0.716$  for DEC,  $R^2 = 0.811$  for EVE). When leaf habit is taken  
337 into account, the scaling for deciduous species can be considered isometric (Fig. S1). By  
338 contrast, evergreen species present an allometric scaling between  $A_x$  and  $A_p$ , with more  
339 xylem produced than phloem (Fig. S1).

340

### 341 *Petiole hydraulic conductivity*

342 Calculated hydraulic conductivity of xylem ( $K_{hx}$ ), i.e., the theoretical capacity of the  
343 whole petiole to supply water to the leaf, results to be positively and significantly ( $P <$   
344  $0.001$ , DEC:  $R^2 = 0.724$ , EVE  $R^2 = 0.560$ ) correlated with LA (Fig. 6a). Deciduous species  
345 with the largest leaves present up to ten-fold higher values of  $K_{hx}$  than the evergreen ones  
346 with the lowest values (Fig. S2a). For both leaf habits an allometric relationship between  
347  $K_{hx}$  and LA is supported (Table 3).

348 The specific conductivity of xylem ( $K_{sx}$ ) also presents a high significance ( $P < 0.001$ ) in  
349 both groups in relation with LA, although correlations are much weaker in comparison to  
350  $K_{hx}$ , especially for evergreen species (DEC:  $R^2 = 0.415$ , EVE:  $R^2 = 0.281$ ) (Fig. 6b, Table  
351 3). Deciduous species present significant higher values of  $K_{sx}$  than evergreen ones (Fig.  
352 S2b). In this case, isometry cannot be rejected for either deciduous or evergreen species  
353 (Table 3). Leaf-specific conductivity (LSC) is significantly higher in deciduous species  
354 than evergreen ones ( $P < 0.001$ ) (Fig. S2c).

355 Calculated phloem hydraulic conductivity ( $K_{hp}$ ) is in all cases much lower than for xylem  
356 with weaker or non-significant correlations with LA (DEC:  $R^2 = 0.276$ ,  $P = 0.06$ ; EVE:  
357  $R^2 = 0.036$ ,  $P = 0.55$ ) (Table 3, plot not shown). It is over 100 times lower than the  $K_{hx}$  on  
358 average for deciduous species (data not shown). Differences among evergreen species are  
359 less remarkable, with a  $K_{hx}$  c.a. 20 times higher than  $K_{hp}$  on average and some specific  
360 individuals with a similar conductivity for both conductive tissues (data not shown).

361 When XLA is compared with the  $K_{sx}$  (Fig. 7a), it can be noticed how deciduous species,  
362 whose leaves are larger, hardly present variation in their XLA values. By contrast they  
363 display a wide range of values in their  $K_s$ . Conversely, evergreen species show a wide  
364 range of variation in their XLA values without an apparent increase in their  $K_{sx}$ , with the  
365 exception of *Q. costaricensis*, which is, in turn, among the species with the largest leaves  
366 within evergreen oaks.

367 Similarly, in the comparison between XLA with the respective  $d_{hx}$  (Fig. 7b), it can be seen  
368 how individuals tend to contribute mainly to one axis depending on their leaf habit. This  
369 is, deciduous species basically present much higher range of variation in  $d_{hx}$  than in XLA.  
370 By contrast, evergreen oaks present a larger variation in XLA than in  $d_{hx}$ . Both increments,  
371 either in  $d_{hx}$  or in XLA leads to an improvement in the LSC, although species that increase  
372 their  $d_{hx}$ , represented by deciduous oaks, improve their LSC more than evergreen oaks  
373 that increase their xylem area.

374

375 *Climatic correlations*

376 Mean annual precipitation reveals a significant relationship with  $d_{hx}$  for evergreen species  
377 ( $P = 0.02$ ) but no significance is found in deciduous ( $P = 0.07$ ). Taking into account the  
378 potential evapotranspiration, i.e., comparing the aridity index (AI) with  $d_{hx}$  improves the  
379 relationships. Aridity index shows positive correlation with  $d_{hx}$  for both deciduous ( $P =$   
380  $0.03$ ;  $R^2 = 0.249$ ) and evergreen species ( $P = 0.02$ ;  $R^2 = 0.274$ ) (Fig. S3). The smallest  
381 hydraulic diameters are displayed in the most xeric species. Regarding temperature, MAT  
382 does not seem to be significantly related to  $d_{hx}$  either for deciduous ( $P = 0.24$ ) or evergreen  
383 species ( $P = 0.91$ ). Conversely,  $T_{min}$  was only compared for evergreen species since  
384 deciduous oaks lack leaves during winter. The correlation did not present significance ( $P$   
385  $= 0.37$ ; Fig. S4).

386

387 *Relationships between vascular traits, stomatal conductance and photosynthesis net rate*

388 When the main attributes of the xylem in the petiole are correlated with the stomatal  
389 conductance at leaf level ( $g_{s,leaf}$ ), significant relationships can be appreciated in all cases  
390 ( $P < 0.001$ ) (Fig. 8). There is a significant increase in  $g_{s,leaf}$  as  $A_x$  becomes larger with an  
391 allometric relationship ( $R^2 = 0.512$ ) (Fig. 8a, Table 4). For a given value of  $A_x$ , deciduous  
392 species tend to present higher values of  $g_{s,leaf}$  than evergreen ones. Stomatal conductance  
393 also increases allometrically as  $d_{hx}$  becomes wider, but with a steeper slope ( $R^2 = 0.586$ )  
394 (Fig. 8b, Table 4). Likewise, deciduous species usually present higher values of  $g_{s,leaf}$  for  
395 the same  $d_{hx}$  than evergreen ones. Once again,  $K_{hx}$  also scaled allometrically (Fig. 8c,  
396 Table 4) and deciduous species have higher values than evergreen species on average.

397 When the same xylem traits are correlated with the photosynthesis net rate, exactly the  
398 same trends arise (Table 4). The  $A_{N,leaf}$  appears to be related to  $A_x$  (Fig. 8d,  $P = 0.001$ ,  $R^2$   
399  $= 0.591$ ),  $d_{hx}$  (Fig. 8e,  $P < 0.001$ ,  $R^2 = 0.671$ ) and  $K_{hx}$  (Fig. 8f,  $P < 0.001$ ,  $R^2 = 0.786$ ).

400 Photosynthesis net rate at leaf level ( $A_{N,leaf}$ ) is significantly correlated with phloem  
401 anatomical traits ( $P < 0.001$ ) (Fig. 9, Table 4).  $A_{N,leaf}$  increases with larger  $A_p$  ( $R^2 = 0.561$ )  
402 (Fig. 9a) and wider  $d_{hp}$  ( $R^2 = 0.509$ ) (Fig. 9b) being on both cases an allometric  
403 relationship. Deciduous species tend to present higher photosynthesis net rates at leaf

404 level than evergreen ones. Finally, the relationship between  $A_{N,leaf}$  and  $K_{hp}$  is barely  
405 significant ( $P = 0.043$ ) with a very weak correlation ( $R^2 = 0.130$ ) (plot not shown).

406

## 407 DISCUSSION

### 408 *Anatomical traits scale with leaf area*

409 In the *Quercus* species studied, we found associations between the anatomical traits of  
410 the petioles and leaf area. First, the cross-sectional area of the petiole displays a rather  
411 scattered association with LA (yet significant). In general, there is an allometric  
412 relationship for deciduous species, whereas evergreen oaks are better adjusted to an  
413 isometric scaling. As we first hypothesized, both hydraulic diameter and conductive area  
414 scale with LA, either as a whole ( $A_c$ ) or separating between xylem ( $A_x$ ) and phloem ( $A_p$ ).  
415 This means that the larger the leaf, the greater the ability for bulk transport of water and  
416 carbohydrates. Increasing the conductivity can be achieved either by increasing the  
417 number of conduits, by producing wider conduits or by a combination of both strategies.  
418 Nonetheless, the scaling becomes weaker in larger leaves.

419 The observed asymptotic response may reflect the different beforementioned constraints  
420 that can compromise the functionality of the conducting tissues. The trade-off between  
421 support and conduction functions of petioles could be explaining the constraint to produce  
422 linearly larger conductive areas in larger leaves. The hydraulic diameter cannot scale  
423 infinitely either. In the xylem, wider conduits are more susceptible to cavitation by both  
424 drought and freezing. For phloem, leaves with wider sieve tube elements would require a  
425 sugar production commensurate with the size of such conduits to generate an adequate  
426 turgor pressure gradient to transport the phloem sap. Otherwise, allocation of sugars  
427 would be hindered. Sieve elements differences can be found depending on the organ, age  
428 and life-form. Thus, stems usually present the widest ones because of the presence of  
429 secondary phloem, in contrast with organs with primary phloem such as leaves or petioles  
430 (Woodruff, 2014; Prislán et al., 2019). Mature trees also present wider sieve elements  
431 than seedlings or saplings (Kopanina et al., 2022). Finally, vines usually develop wider  
432 sieve elements than free-standing plants, since they do not need as much support tissue  
433 as a tree (Ewers and Fisher, 1991; Losada et al., 2022). Despite these differences,  
434 interspecific variation of sieve element diameter is lower than for xylem vessel diameter,  
435 which agrees with our results. Thus, the limitations imposed to phloem seem to be more

436 restrictive than those imposed to xylem. This makes sense if we consider that maintaining  
437 the proper function of phloem is more critical than xylem for several reasons. First,  
438 phloem sap flows during the whole day, night included, in contrast to xylem flow, which  
439 reaches the highest values when stomata are opened during the day. Second, phloem must  
440 maintain a constant turgor to achieve a steady flow since either an excessive viscosity or  
441 a loss of turgor level will hinder the sap flow (Lang, 1978).

442 The scaling relationship between xylem and phloem areas has been also explored in  
443 several studies (Table 5), which find an isometric scaling between  $A_x$  and  $A_p$ . Nonetheless,  
444 most of these studies only focus on single species. Our work clearly improves this by  
445 exploring the scaling relationship in a great number of species, closely related but  
446 different enough in leaf habit and climatic ranges. Our data support an isometric scaling  
447 in the case of deciduous species, but an allometric scaling between xylem and phloem in  
448 evergreen species, favoring more production of xylem than phloem area (Fig. S1), which  
449 reflects the higher values of XLA in evergreen species (see next section for further  
450 details). A scaling relationship between the conductive areas in any case should be  
451 expected, since both tissues are originated from the same meristematic tissue, i.e., the  
452 procambium. In addition, despite having very different function, xylem and phloem are  
453 interconnected. The main hydric relationship relies on xylem supplying water to load  
454 phloem companion cells and sieve tubes according to a lateral water potential gradient  
455 between both tissues. The flux of sugars depends on the product of water flux and sugar  
456 concentration. Since the sugar concentration declines with distance from the leaf, water  
457 flux must increase to keep the sap flux steady. In other words, there is an influx of water  
458 from the xylem throughout the transport phloem to compensate for the lower sugar  
459 concentrations. The balanced interaction between xylem and phloem is an essential  
460 requirement for long-distance transport (Dinant and Lemoine, 2010; Sevanto, 2014).

461 Concerning the hydraulic conductivity after applying Hagen-Poiseuille law, we reported  
462 an improvement in xylem  $K_h$  with LA, due to the combination of both a larger  $A_x$  and  
463 wider  $d_h$ . This increment in xylem efficiency is still reflected even after removing the  
464 effect of developing more  $A_x$  due to larger leaf areas, i.e., the  $K_{sx}$ . However, this is not the  
465 case for phloem, where the dispersion of the data is much higher (Table 3). Here, solely  
466 diameter of the phloem cells does not seem to predict the actual hydraulic conductivity  
467 of phloem by itself, probably due to a mix of cellular types in the measurements. In  
468 addition, some other factors related to the nature of sieve plates, such as the number of

469 pores, diameter of such pores and even number of plates per sieve element, are likely to  
470 modulate the hydraulic conductivity of phloem.

471

472 *Deciduous and evergreen oaks follow different strategies producing and packaging their*  
473 *conduits*

474 The main differences between deciduous and evergreen oak species arise when we  
475 compare the conductive area standardized by LA (i.e., the XLA) with the  $K_{sx}$  and  $d_{hx}$  (Fig.  
476 7). In this scenario, the range of variation in both  $K_{sx}$  and  $d_{hx}$  mainly corresponds with  
477 deciduous species, whereas the range of variation in XLA mostly corresponds with  
478 evergreen species. The larger LA of deciduous oaks requires a higher water supply which  
479 is, in turn, reflected by a higher photosynthetic rate and stomatal conductance compared  
480 to evergreen species. Thus, deciduous species display up to an order of magnitude higher  
481  $K_{sx}$  values than evergreen oaks. An increase in  $K_{sx}$  can be achieved either by reducing the  
482 xylem area or by widening the xylem vessels for the same size and number of vessels,  
483 which ultimately increases  $K_{hx}$ . Since the xylem area increases with LA, this increase in  
484  $K_{sx}$  in deciduous species can only be modulated by an increase in the diameter of the  
485 xylem vessels. By contrast, evergreen oaks hardly present range of variation in their  $K_{sx}$   
486 values, with the exception of *Q. costaricensis*, the evergreen oak with the widest vessels  
487 in this study.

488 Subsequently, we compared  $d_{hx}$  with XLA, but this time transforming  $K_{sx}$  into a more  
489 physiologically meaningful variable, that is LSC, which links the capacity of xylem to  
490 transport water with the leaf water demands (Mencuccini et al., 2019). In this correlation  
491 (Fig. 7b), deciduous oaks always present low XLA values, close to or lower than one, but  
492 they display a wide range of variation in their  $d_{hx}$ . Conversely, evergreen oaks exhibit a  
493 wider variation in their XLA values but narrower  $d_{hx}$  values. In other words, deciduous  
494 species tend to produce wider conduits to improve their xylem hydraulic conductivity for  
495 a given leaf area, whereas evergreen species choose to increase their  $A_x$  for the same leaf  
496 area over the  $d_h$ .

497 This dichotomous strategy between deciduous (Fig. 1, Model A) and evergreen (Fig. 1,  
498 Model B) oaks could be directly related with both, their leaf life spans and the climatic  
499 niches they occupy. First, deciduous leaves only have to keep functional for a few months  
500 (typically 6-9 months). Thus, they can take a riskier but, simultaneously, a more effective



501 —showed by high LSC values— and a cheaper strategy (Ni et al., 2022). On the other  
502 hand, evergreen species, whose leaves must remain productive for longer periods, tend to  
503 follow a safer strategy at the expense of a more costly investment (Hacke et al., 2000).  
504 Nonetheless, this investment in larger  $A_x$  also increases the LSC in those species with high  
505 values of XLA, partly counterbalancing their lower  $K_{hx}$  values and reaching efficiencies  
506 close to deciduous species. Besides, this safer strategy could be the main contributor to  
507 the allometry found in xylem for evergreen species in comparison to the isometry that  
508 most studies find and is also present in our deciduous species.

509 Second, deciduous oaks considered in this study are mainly represented by species  
510 occupying temperate forests. These habitats rarely present stressful conditions (drought  
511 and/or cold) during the lifespan of the leaves (Peguero-Pina et al., 2016). Hence, it is  
512 reasonable to think that deciduous oaks could afford more efficient vessels at the expense  
513 of more vulnerability. Accordingly, most of the evergreen oak species (with the exception  
514 of some tropical ones; e.g., *Q. costaricensis*) must cope with at least one stressful period  
515 during the year (typically a drought period), and even two in the case of Mediterranean  
516 species (summer drought and winter cold) (Martín-Sánchez et al., 2022). Therefore, it is  
517 justifiable to consider that these species choose a conservative strategy for building their  
518 conductive tissues. Furthermore, deciduous oaks occupying extra-temperate habitats with  
519 stressful periods such as the Mediterranean Basin (e.g., *Q. faginea* and *Q. ithaburensis*)  
520 or winter-dry temperate climates in Mexico (e.g., *Q. crassipes*) present the smallest values  
521 of both leaf area and hydraulic diameter among deciduous oaks, suggesting the reduction  
522 of xylem vessels in environmental restrictive habitats. Indeed, aridity index shows  
523 correlation with  $d_{hx}$  for both deciduous and evergreen species. The more xeric the climate  
524 is, the narrower the xylem vessels are. This relationship between drought and vessel size  
525 has been widely reported by numerous authors in stems, branches and leaves, resulting in  
526 a trade-off between efficiency and safety (Hajek et al., 2014; Pivovarovoff et al., 2016;  
527 Schreibet et al., 2016; Barotto et al., 2017). It has also been recently found in petioles by  
528 comparing XLA and resistance to cavitation in several *Eucalyptus* species (Blackman et  
529 al., 2023). Likewise, this compensation of improving the hydraulic conductivity by  
530 increasing the conductive area over the diameters of the conduits has been also reported  
531 in stems of several species (Nardini et al., 2012) but, to our knowledge, it has never been  
532 attributed to leaf habit in any case.

533 We demonstrate the presence of two models for producing and packaging the conduits,  
534 and we also prove the relationship between aridity and hydraulic diameter. However, we  
535 did not find significant correlation between cold, here represented by the WorldClim2  
536 variable “mean of daily minimum temperatures during the coldest quarter”, and  $d_{hx}$  in  
537 evergreen oaks. Nonetheless, cavitation induced by winter cold is caused by freeze-thaw  
538 cycles, a climatic variable for which global-scale data are not available. The lack of  
539 significance is mainly due to two species: *Q. semecarpifolia* and *Q. engleriana*. These  
540 evergreen species present a wide range of distribution in Asia, in habitats that present a  
541 complex orography, resulting in very different climatic conditions. A detailed study in  
542 their natural habitats along altitudinal and climatic gradients, measuring the daily  
543 temperatures, might reveal a reduction in  $d_{hx}$  in those sites where trees have to withstand  
544 more frequent freeze-thaw cycles. Other species, such as *Q. chrysolepis* and *Q.*  
545 *monimotricha*, for instance, the two species with the narrowest vessels, can be found in  
546 very high-altitude habitats, where they are exposed to recurrent frosts during the coldest  
547 months. Thus, according to the leaf economic spectrum, these species would not recover  
548 the investment in case such expensive leaves died earlier due to a hydraulic failure. By  
549 contrast, evergreen species with the widest vessels (e.g. *Q. costaricensis*, *Q. virginiana*)  
550 occupy tropical or subtropical habitats with the absence of strong and frequent frosts.

551

#### 552 *Anatomy of petioles accommodates physiological demands*

553 Our data supports a strong correlation between the petiole anatomical traits of both, xylem  
554 and phloem, and the estimated  $g_s$  and  $A_N$  at leaf-level. The strongest relationships are  
555 found between xylem traits and  $A_{N,leaf}$ , albeit xylem- $g_{s,leaf}$  correlations shows similar  
556 statistical power. Even though Figures 8 and 9 represent deciduous and evergreen species  
557 in different colours, the aim is not to see differences in leaf habit but explore the  
558 anatomical architecture in response to the physiological demands of the leaf lamina. This  
559 link function-structure has been proposed to be mediated throughout several  
560 physiological processes, such as water potential, hydraulic conductance, turgor pressure  
561 or sugar concentration (Hölttä et al., 2010). These factors would have an effect on the  
562 ontogeny and development of the cells in a tissue (Cosgrove, 1993).

563 Relationships between xylem area in the petiole and leaf transpiration were proposed  
564 more than one hundred years ago by Salisbury (1913). However, this author suggested

565 that the nature of the conduits —i.e., number and size— should receive more attention.  
566 Here, we explore not only such relationship between  $A_x$  and  $g_{s,leaf}$ , but also the size of the  
567 conduits and the calculated  $K_{hx}$ , which all resulted to be highly correlated with  $g_{s,leaf}$ .  
568 Brocious and Hacke (2016), presented a study among different *Populus* hybrids where no  
569 differences among several clones were found, however, when all leaves were analyzed  
570 together, they found similar trends to our findings for  $A_x$  and  $K_{hx}$  in relation to  $g_s$ ,  
571 suggesting that ‘lamina size is constrained by the transport capacity of the vascular tissue  
572 in the petiole’. Concerning the scaling relationship, our results show an allometry in all  
573 cases. In this regard, Zhong et al. (2020) also found allometric scaling in 53 woody  
574 species between xylem area in the midrib and the number of stomata in the leaf lamina,  
575 but they reported an isometric scaling of leaf area and total stomatal area. Nonetheless, it  
576 must not be disregarded that stomatal conductance is only showing the capacity of  
577 stomata to release water to atmosphere, but the transpiration rate is the variable actually  
578 measuring water losses in leaves by taking into account the vapor pressure deficit (VPD).  
579 In this context, part of the scatter observed in the association between petiole xylem traits  
580 and  $g_{s,leaf}$  might be attributed to adaptations to different VPD levels during the growing  
581 season.

582 A higher photosynthetic rate is related to a larger xylem hydraulic conductance because  
583 of a greater water usage (Brodribb and Field, 2000; Hölttä et al., 2010). The largest leaves  
584 among our species correspond with deciduous species, and they present a higher  $A_{N,leaf}$   
585 compared to evergreen species. However, when  $A_N$  —expressed in  $m^2$ — is compared, no  
586 significant differences linked to leaf habit are found (Peguero-Pina et al., 2017). In this  
587 case, taking into account the total photosynthesis rate at leaf level is more logical than  
588 standardizing it for a given area because a petiole must have an anatomical structure able  
589 to export the sucrose produced by the leaf. Sucrose is the most abundant photosynthate  
590 transported by sieve elements, but viscosity of a sucrose solution increases exponentially  
591 with increasing concentration (Morison, 2002). Furthermore, the viscosity of the sap is  
592 one of the main factors that limit phloem transport, since the more viscous the solution,  
593 the lower the flow rate (Lang, 1978; Sevanto, 2014). To deal with this disadvantage, plants  
594 can choose between two strategies. On the one hand, sink organs could lower their sugar  
595 concentration, increasing the source-sink concentration gradient. On the other hand, they  
596 could develop wider sieve tubes, since an increment in the radius of a sieve tube should  
597 improve the hydraulic conductivity to the fourth power. This latter strategy seems to be

598 more feasible for the plant (Hölttä et al., 2009; Sevanto, 2014). Thus, the largest leaves in  
599 oak species, which are in turn the ones which produce more sucrose, would need wider  
600 sieve tubes to avoid a depleted flow rate caused by an excessive viscosity.

601

## 602 CONCLUSION

603 The conductive tissues in the petiole scale allometrically with leaf area, which ultimately  
604 reflects the demands on the leaf. Xylem and phloem present a very similar pattern in their  
605 scaling both for conductive areas and for the diameters of their cells. Although increasing  
606 the diameter of the conduits would imply a greater improvement in the hydraulic  
607 conductivity than increasing the conductive area, it also results in a riskier strategy. For  
608 this reason, a coordinated scaling between both alternatives is required depending on the  
609 habitat occupied by the species. For example, species inhabiting arid habitats tend to have  
610 narrower conduits than those species occupying cool nemoral habitats.

611 We find that oaks with different leaf habits tend to improve their hydraulic conductivities  
612 with two contrasting approaches. Deciduous species opt to produce wider vessels for the  
613 same conductive and leaf areas compared to evergreen oaks. Conversely, evergreen  
614 species choose to increase their conductive area over the diameter of the conduits.

615 Most studies inquiring into the scaling between xylem and phloem find isometric  
616 relationships. Deciduous oaks exhibit the same isometric pattern. However, evergreen  
617 species present an allometric scaling, producing more xylem than phloem, which agrees  
618 with their safer strategy.

619 Phloem is more constrained than xylem in increasing the diameter of its main conduits.  
620 This is probably related to the very different functionality of both tissues. While xylem  
621 mainly responds to water demands during the photosynthesis, phloem is responsible for  
622 maintaining a proper balance of sugars, hormones and other metabolites throughout the  
623 plant and throughout the day.

624 The structure of the conductive tissues straightly corresponds with leaf demands. Xylem  
625 area, vessel size and hydraulic conductivity in the petiole are correlated with both  
626 photosynthesis net rate and stomatal conductance at leaf level. Phloem anatomy also  
627 relates to photosynthesis rate.

628

629 ACKNOWLEDGEMENTS

630 We thank Jardín Botánico de Iturrarán and Francisco Garín for allowing us to collect oak  
631 leaf samples from their garden. This research was supported by Grant PID2022-  
632 136478OB-C32 funded by MICIU/AEI/10.13039/501100011033 and by “ERDF A way  
633 of making Europe”, by grant CNS2022-136156 funded by  
634 MCIN/AEI/10.13039/501100011033 and European Union Next Generation EU/PRTR  
635 and by Gobierno de Aragón S74\_23R research group. The work of Rubén Martín-  
636 Sánchez was supported by a PhD Gobierno de Aragón scholarship.

637

638 DATA AVAILABILITY STATEMENT

639 The data that supports the findings of this study are available in  
640 <https://doi.org/https://doi.org/10.5281/zenodo.12730852>.

641 REFERENCES

- 642 1. Alonso-Forn, D., Sancho-Knapik, D., Ferrio, J. P., Peguero-Pina, J. J., Bueno,  
643 A., Onoda, Y., Cavender-bares, J., Niinemets, Ü., Jansen, S., Riederer, M.,  
644 Cornelissen, J.H.C., Chai, Y., & Gil-Pelegrín, E. (2020). Revisiting the  
645 functional basis of sclerophylly within the leaf economics spectrum of oaks:  
646 different roads to Rome. *Current Forestry Reports*, 6(4), 260-281.  
647 <https://doi.org/10.1007/s40725-020-00122-7>.
- 648 2. Alonso-Forn, D., Peguero-Pina, J. J., Ferrio, J. P., Mencuccini, M., Mendoza-  
649 Herrer, Ó., Sancho-Knapik, D., & Gil-Pelegrín, E. (2021). Contrasting  
650 functional strategies following severe drought in two Mediterranean oaks with  
651 different leaf habit: *Quercus faginea* and *Quercus ilex* subsp. *rotundifolia*. *Tree*  
652 *Physiology*, 41(3), 371-387. <https://doi.org/10.1093/treephys/tpaa135>.
- 653 3. Barotto, A. J., Monteoliva, S., Gyenge, J., Martinez-Meier, A., & Fernandez,  
654 M. E. (2018). Functional relationships between wood structure and  
655 vulnerability to xylem cavitation in races of *Eucalyptus globulus* differing in  
656 wood density. *Tree Physiology*, 38(2), 243-251.  
657 <https://doi.org/10.1093/treephys/tpx138>.
- 658 4. Blackman, C. J., Halliwell, B., Hartill, G. E., & Brodribb, T. J. (2024). Petiole  
659 XLA (xylem to leaf area ratio) integrates hydraulic safety and efficiency across  
660 a diverse group of eucalypt leaves. *Plant, Cell & Environment*, 47(1), 49-58.  
661 <https://doi.org/10.1111/pce.14713>.
- 662 5. Brocious, C. A., & Hacke, U. G. (2016). Stomatal conductance scales with  
663 petiole xylem traits in *Populus* genotypes. *Functional Plant Biology*, 43(6),  
664 553-562. <https://doi.org/10.1071/FP15336>.
- 665 6. Brodribb, T. J., & Feild, T. S. (2000). Stem hydraulic supply is linked to leaf  
666 photosynthetic capacity: evidence from New Caledonian and Tasmanian  
667 rainforests. *Plant, Cell & Environment*, 23(12), 1381-1388.  
668 <https://doi.org/10.1046/j.1365-3040.2000.00647.x>.
- 669 7. Cai, J., & Tyree, M. T. (2010). The impact of vessel size on vulnerability  
670 curves: data and models for within-species variability in saplings of aspen,  
671 *Populus tremuloides* Michx. *Plant, Cell & Environment*, 33(7), 1059-1069.  
672 <https://doi.org/10.1111/j.1365-3040.2010.02127.x>.

- 673 8. Carvalho, M. R., Turgeon, R., Owens, T., & Niklas, K. J. (2017a). The scaling  
674 of the hydraulic architecture in poplar leaves. *New Phytologist*, 214(1), 145-  
675 157. <https://doi.org/10.1111/nph.14385>.
- 676 9. Carvalho, M. R., Turgeon, R., Owens, T., & Niklas, K. J. (2017b). The  
677 hydraulic architecture of Ginkgo leaves. *American Journal of Botany*, 104(9),  
678 1285-1298. <https://doi.org/10.3732/ajb.1700277>.
- 679 10. Cochard, H., & Tyree, M. T. (1990). Xylem dysfunction in *Quercus*: vessel  
680 sizes, tyloses, cavitation and seasonal changes in embolism. *Tree physiology*,  
681 6(4), 393-407. <https://doi.org/10.1093/treephys/6.4.393>.
- 682 11. Cosgrove, D. J. (1993). Wall extensibility: its nature, measurement and  
683 relationship to plant cell growth. *New Phytologist*, 124(1), 1-23.  
684 <https://doi.org/10.1111/j.1469-8137.1993.tb03795.x>.
- 685 12. Dinant, S., & Lemoine, R. (2010). The phloem pathway: new issues and old  
686 debates. *Comptes Rendus Biologies*, 333(4), 307-319.  
687 <https://doi.org/10.1071/PP9780535>.
- 688 13. Esau, K. (1939). Development and structure of the phloem tissue. *The*  
689 *Botanical Review*, 5, 373-432. <https://doi.org/10.1007/BF02878295>.
- 690 14. Ewers, F. W., & Fisher, J. B. (1991). Why vines have narrow stems:  
691 histological trends in *Bauhinia* (Fabaceae). *Oecologia*, 88, 233-237.  
692 <https://doi.org/10.1007/BF00320816>.
- 693 15. Fick, S.E. & R.J. Hijmans, (2017). WorldClim 2: new 1km spatial resolution  
694 climate surfaces for global land areas. *International Journal of Climatology*,  
695 37 (12), 4302-4315.
- 696 16. Gil-Pelegrín, E., Saz, M.Á., Cuadrat, J.M., Peguero-Pina, J.J., Sancho-Knapik,  
697 D. (2017). Oaks Under Mediterranean-Type Climates: Functional Response to  
698 Summer Aridity. In: Gil-Pelegrín, E., Peguero-Pina, J., Sancho-Knapik, D.  
699 (eds) *Oaks Physiological Ecology. Exploring the Functional Diversity of*  
700 *Genus Quercus L.. Tree Physiology*, vol 7. Springer, Cham.  
701 [https://doi.org/10.1007/978-3-319-69099-5\\_5](https://doi.org/10.1007/978-3-319-69099-5_5).
- 702 17. Giordano, R., Salleo, A., Salleo, S., & Wanderlingh, F. (1978). Flow in xylem  
703 vessels and Poiseuille's law. *Canadian Journal of Botany*, 56(3), 333-338.  
704 <https://doi.org/10.1139/b78-039>.
- 705 18. Gleason, S. M., Blackman, C. J., Chang, Y., Cook, A. M., Laws, C. A., &  
706 Westoby, M. (2016). Weak coordination among petiole, leaf, vein, and gas-

- 707 exchange traits across Australian angiosperm species and its possible  
708 implications. *Ecology and Evolution*, 6(1), 267-278.  
709 <https://doi.org/10.1002/ece3.1860>.
- 710 19. Hacke, U., & Sauter, J. J. (1996). Drought-induced xylem dysfunction in  
711 petioles, branches, and roots of *Populus balsamifera* L. and *Alnus glutinosa*  
712 (L.) Gaertn. *Plant Physiology*, 111(2), 413-417.  
713 <https://doi.org/10.1104/pp.111.2.413>
- 714 20. Hacke, U. G., Sperry, J. S., & Pittermann, J. (2000). Drought experience and  
715 cavitation resistance in six shrubs from the Great Basin, Utah. *Basic and*  
716 *Applied Ecology*, 1(1), 31-41. <https://doi.org/10.1078/1439-1791-00006>.
- 717 21. Hacke, U. G., Sperry, J. S., Wheeler, J. K., & Castro, L. (2006). Scaling of  
718 angiosperm xylem structure with safety and efficiency. *Tree physiology*, 26(6),  
719 689-701. <https://doi.org/10.1093/treephys/26.6.689>.
- 720 22. Hajek, P., Leuschner, C., Hertel, D., Delzon, S., & Schuldt, B. (2014). Trade-  
721 offs between xylem hydraulic properties, wood anatomy and yield in *Populus*.  
722 *Tree physiology*, 34(7), 744-756. <https://doi.org/10.1093/treephys/tpu048>.
- 723 23. Harayama, H., Ishida, A., & Yoshimura, J. (2016). Overwintering evergreen  
724 oaks reverse typical relationships between leaf traits in a species spectrum.  
725 *Royal Society Open Science*, 3(7), 160276.  
726 <https://doi.org/10.1098/rsos.160276>.
- 727 24. Hartig F. (2022). DHARMa: Residual Diagnostics for Hierarchical (Multi-  
728 Level / Mixed) Regression Models. R package version 0.4.6. [https://cran.r-](https://cran.r-project.org/web/packages/DHARMa)  
729 [project.org/web/packages/DHARMa](https://cran.r-project.org/web/packages/DHARMa).
- 730 25. Hirose, S., Kume, A., Takeuchi, S., Utsumi, Y., Otsuki, K., & Ogawa, S.  
731 (2005). Stem water transport of *Lithocarpus edulis*, an evergreen oak with  
732 radial-porous wood. *Tree physiology*, 25(2), 221-  
733 228. <https://doi.org/10.1093/treephys/25.2.221>.
- 734 26. Hölttä, T., Mäkinen, H., Nöjd, P., Mäkelä, A., & Nikinmaa, E. (2010). A  
735 physiological model of softwood cambial growth. *Tree Physiology*, 30(10),  
736 1235-1252. <https://doi.org/10.1093/treephys/tpq068>.
- 737 27. Hölttä, T., Mencuccini, M., & Nikinmaa, E. (2009). Linking phloem function  
738 to structure: analysis with a coupled xylem–phloem transport model. *Journal*  
739 *of theoretical biology*, 259(2), 325-337.  
740 <https://doi.org/10.1016/j.jtbi.2009.03.039>.



- 741 28. Huang, W., Hu, H., & Zhang, S. B. (2016). Photosynthesis and photosynthetic  
742 electron flow in the alpine evergreen species *Quercus guyavifolia* in winter.  
743 *Frontiers in Plant Science*, 7, 204522.  
744 <https://doi.org/10.3389/fpls.2016.01511>.
- 745 29. Jacobsen, A. L., Pratt, R. B., Venturas, M. D., & Hacke, U. G. (2019). Large  
746 volume vessels are vulnerable to water-stress-induced embolism in stems of  
747 poplar. *IAWA journal*, 40(1), 4-S4. [https://doi.org/10.1163/22941932-](https://doi.org/10.1163/22941932-40190233)  
748 [40190233](https://doi.org/10.1163/22941932-40190233).
- 749 30. Jafarnia, S., Akbarinia, M., Hosseinpour, B., Modarres Sanavi, S. A. M., &  
750 Salami, S. A. (2018). Effect of drought stress on some growth, morphological,  
751 physiological, and biochemical parameters of two different populations of  
752 *Quercus brantii*. *iForest-Biogeosciences and Forestry*, 11(2), 212.  
753 <https://doi.org/10.3832/ifor2496-010>.
- 754 31. Jensen, K. H., Savage, J. A., & Holbrook, N. M. (2013). Optimal concentration  
755 for sugar transport in plants. *Journal of the Royal Society Interface*, 10(83),  
756 20130055. <https://doi.org/10.1098/rsif.2013.0055>.
- 757 32. Jyske, T., & Hölttä, T. (2015). Comparison of phloem and xylem hydraulic  
758 architecture in *Picea abies* stems. *New phytologist*, 205(1), 102-115.  
759 <https://doi.org/10.1111/nph.12973>.
- 760 33. Kar, S., Montague, D. T., & Villanueva-Morales, A. (2021). Measurement of  
761 photosynthesis in excised leaves of ornamental trees: a novel method to  
762 estimate leaf level drought tolerance and increase experimental sample size.  
763 *Trees*, 35, 889-905. [10.1111/j.2041-210X.2011.00153.x](https://doi.org/10.1111/j.2041-210X.2011.00153.x)  
764 [10.1007/s00468-021-02088-w](https://doi.org/10.1111/j.2041-210X.2011.00153.x).
- 765 34. Kikuzawa, K., Onoda, Y., Wright, I. J., & Reich, P. B. (2013). Mechanisms  
766 underlying global temperature-related patterns in leaf longevity. *Global  
767 Ecology and Biogeography*, 22(8), 982-993.  
768 <https://doi.org/10.1111/geb.12042>.
- 769 35. Kiorapostolou, N., & Petit, G. (2019). Similarities and differences in the  
770 balances between leaf, xylem and phloem structures in *Fraxinus ornus* along  
771 an environmental gradient. *Tree Physiology*, 39(2), 234-242.  
772 <https://doi.org/10.1093/treephys/tpy095>.
- 773 36. Kopanina, A. V., Talskikh, A. I., Vlasova, I. I., & Kotina, E. L. (2022). Age-  
774 related pattern in bark formation of *Betula ermanii* growing in volcanic

- 775 environments from southern Sakhalin and Kuril Islands (Northeast Asia).  
776 *Trees*, 36(3), 915-939. <https://doi.org/10.1007/s00468-021-02257-x>.
- 777 37. Lang, A. (1978). A model of mass flow in the phloem. *Functional Plant*  
778 *Biology*, 5(4), 535-546. <https://doi.org/10.1071/PP9780535>.
- 779 38. Lemoine, D., Granier, A., & Cochard, H. (1999). Mechanism of freeze-  
780 induced embolism in *Fagus sylvatica* L. *Trees*, 13, 206-210.  
781 <https://doi.org/10.1007/PL00009751>.
- 782 39. Llusia, J., Roahtyn, S., Yakir, D., Rotenberg, E., Seco, R., Guenther, A., &  
783 Penuelas, J. (2016). Photosynthesis, stomatal conductance and terpene  
784 emission response to water availability in dry and mesic Mediterranean  
785 forests. *Trees*, 30, 749-759. <https://doi.org/10.1007/s00468-015-1317-x>.
- 786 40. Lo Gullo, M. A., & Salleo, S. (1993). Different vulnerabilities of *Quercus ilex*  
787 L. to freeze-and summer drought-induced xylem embolism: an ecological  
788 interpretation. *Plant, Cell & Environment*, 16(5), 511-519.  
789 <https://doi.org/10.1111/j.1365-3040.1993.tb00898.x>.
- 790 41. Losada, J. M., He, Z., & Holbrook, N. M. (2022). Sieve tube structural  
791 variation in *Austrobaileya scandens* and its significance for lianescence. *Plant,*  
792 *Cell & Environment*, 45(8), 2460-2475. <https://doi.org/10.1111/pce.14361>.
- 793 42. Martín-Sánchez, R., Peguero-Pina, J. J., Alonso-Forn, D., Ferrio, J. P., Sancho-  
794 Knapik, D., & Gil-Peigrín, E. (2022). Summer and winter can equally stress  
795 holm oak (*Quercus ilex* L.) in Mediterranean areas: a physiological view.  
796 *Flora*, 290, 152058. <https://doi.org/10.1016/j.flora.2022.152058>.
- 797 43. Martín-Sánchez, R., Sancho-Knapik, D., Alonso-Forn, D., López-Ballesteros,  
798 A., Ferrio, J. P., Hipp, A. L., Peguero-Pina, J.J., & Gil-Peigrín, E. (2024). Oak  
799 leaf morphology may be more strongly shaped by climate than by phylogeny.  
800 *Annals of Forest Science*, 81(1), 14. [https://doi.org/10.1186/s13595-024-](https://doi.org/10.1186/s13595-024-01232-z)  
801 [01232-z](https://doi.org/10.1186/s13595-024-01232-z).
- 802 44. Mediavilla, S., García-Ciudad, A., García-Criado, B., & Escudero, A. (2008).  
803 Testing the correlations between leaf life span and leaf structural  
804 reinforcement in 13 species of European Mediterranean woody plants.  
805 *Functional Ecology*, 22(5), 787-793. [https://doi.org/10.1111/j.1365-](https://doi.org/10.1111/j.1365-2435.2008.01453.x)  
806 [2435.2008.01453.x](https://doi.org/10.1111/j.1365-2435.2008.01453.x).
- 807 45. Mencuccini, M., Rosas, T., Rowland, L., Choat, B., Cornelissen, H., Jansen,  
808 S., ... & Martínez-Vilalta, J. (2019). Leaf economics and plant hydraulics drive

- 809 leaf: wood area ratios. *New Phytologist*, 224(4), 1544-1556.  
810 <https://doi.org/10.1111/nph.15998>.
- 811 46. Morison, K. R. (2002). Viscosity equations for sucrose solutions: old and new  
812 2002. In *Proceedings of the 9th APCChE Congress and CHEMECA*.
- 813 47. Nagel, J. M., Griffin, K. L., Schuster, W. S., Tissue, D. T., Turnbull, M. H.,  
814 Brown, K. J., & Whitehead, D. (2002). Energy investment in leaves of red  
815 maple and co-occurring oaks within a forested watershed. *Tree Physiology*,  
816 22(12), 859-867. <https://doi.org/10.1093/treephys/22.12.859>.
- 817 48. Nardini, A., Pedà, G., & La Rocca, N. (2012). Trade-offs between leaf  
818 hydraulic capacity and drought vulnerability: morpho-anatomical bases,  
819 carbon costs and ecological consequences. *New Phytologist*, 196(3), 788-798.  
820 <https://doi.org/10.1111/j.1469-8137.2012.04294.x>.
- 821 49. Ni, X., Sun, L., Cai, Q., Ma, S., Feng, Y., Sun, Y., An, L., & Ji, C. (2022).  
822 Variation and determinants of leaf anatomical traits from boreal to tropical  
823 forests in eastern China. *Ecological Indicators*, 140, 108992.  
824 <https://doi.org/10.1016/j.ecolind.2022.108992>.
- 825 50. Peguero-Pina, J. J., Sancho-Knapik, D., Martín, P., Saz, M. Á., Gea-Izquierdo,  
826 G., Cañellas, I., & Gil-Pelegrín, E. (2015). Evidence of vulnerability  
827 segmentation in a deciduous Mediterranean oak (*Quercus subpyrenaica* EH  
828 del Villar). *Trees*, 29, 1917-1927. <https://doi.org/10.1007/s00468-015-1273-5>.
- 829 51. Peguero-Pina, J. J., Sisó, S., Sancho-Knapik, D., Díaz-Espejo, A., Flexas, J.,  
830 Galmés, J., & Gil-Pelegrín, E. (2016). Leaf morphological and physiological  
831 adaptations of a deciduous oak (*Quercus faginea* Lam.) to the Mediterranean  
832 climate: a comparison with a closely related temperate species (*Quercus robur*  
833 L.). *Tree Physiology*, 36(3), 287-299. <https://doi.org/10.1093/treephys/tpv107>.
- 834 52. Peguero-Pina, J. J., Aranda, I., Cano, F. J., Galmés, J., Gil-Pelegrín, E.,  
835 Niinemets, Ü., Sancho-Knapik, D., & Flexas, J. (2017). The role of mesophyll  
836 conductance in oak photosynthesis: among-and within-species variability. In:  
837 Gil-Pelegrín, E., Peguero-Pina, J., Sancho-Knapik, D. (eds) *Oaks*  
838 *Physiological Ecology. Exploring the Functional Diversity of Genus Quercus*  
839 *L.. Tree Physiology*, vol 7. Springer, Cham. [https://doi.org/10.1007/978-3-](https://doi.org/10.1007/978-3-319-69099-5_9)  
840 [319-69099-5\\_9](https://doi.org/10.1007/978-3-319-69099-5_9).
- 841 53. Peguero-Pina, J. J., Vilagrosa, A., Alonso-Forn, D., Ferrio, J. P., Sancho-  
842 Knapik, D., & Gil-Pelegrín, E. (2020). Living in drylands: Functional

- 843 adaptations of trees and shrubs to cope with high temperatures and water  
844 scarcity. *Forests*, 11(10), 1028. <https://doi.org/10.3390/f11101028>.
- 845 54. Pivovarov, A. L., Pasquini, S. C., De Guzman, M. E., Alstad, K. P., Stemke,  
846 J. S., & Santiago, L. S. (2016). Multiple strategies for drought survival among  
847 woody plant species. *Functional Ecology*, 30(4), 517-526.  
848 <https://doi.org/10.1111/1365-2435.12518>.
- 849 55. Prislán, P., Mrak, P., Žnidaršič, N., Štrus, J., Humar, M., Thaler, N., Mrak, T.,  
850 & Gričar, J. (2019). Intra-annual dynamics of phloem formation and  
851 ultrastructural changes in sieve tubes in *Fagus sylvatica*. *Tree Physiology*,  
852 39(2), 262-274. <https://doi.org/10.1093/treephys/tpy102>.
- 853 56. Ray, D. M., & Jones, C. S. (2018). Scaling relationships and vessel packing in  
854 petioles. *American Journal of Botany*, 105(4), 667-676.  
855 <https://doi.org/10.1002/ajb2.1054>.
- 856 57. Salisbury, E. J. (1913). The determining factors in petiolar structure. *New*  
857 *Phytologist*, 12(8), 281-289.
- 858 58. Sancho-Knapik, D., Escudero, A., Mediavilla, S., Scoffoni, C., Zailaa, J.,  
859 Cavender-Bares, J., Álvarez-Arenas, T.G., Molins, A., Alonso-Forn, D.,  
860 Ferrio, J.P., Peguero-Pina, J.J., & Gil-Pelegrín, E. (2021). Deciduous and  
861 evergreen oaks show contrasting adaptive responses in leaf mass per area  
862 across environments. *New Phytologist*, 230(2), 521-534.  
863 <https://doi.org/10.1111/nph.17151>.
- 864 59. Schreiber, S. G., Hacke, U. G., Chamberland, S., Lowe, C. W., Kamelchuk,  
865 D., Bräutigam, K., ... & Thomas, B. R. (2016). Leaf size serves as a proxy for  
866 xylem vulnerability to cavitation in plantation trees. *Plant, Cell &*  
867 *Environment*, 39(2), 272-281. <https://doi.org/10.1111/pce.12611>.
- 868 60. Sevanto, S. (2014). Phloem transport and drought. *Journal of experimental*  
869 *botany*, 65(7), 1751-1759. <https://doi.org/10.1093/jxb/ert467>.
- 870 61. Sevanto, S., Holbrook, N. M., & Ball, M. C. (2012). Freeze/thaw-induced  
871 embolism: probability of critical bubble formation depends on speed of ice  
872 formation. *Frontiers in Plant Science*, 3, 107.  
873 <https://doi.org/10.3389/fpls.2012.00107>.
- 874 62. Sperry, J. S., & Sullivan, J. E. (1992). Xylem embolism in response to freeze-  
875 thaw cycles and water stress in ring-porous, diffuse-porous, and conifer

- 876 species. *Plant physiology*, 100(2), 605-613.  
877 <https://doi.org/10.1104/pp.100.2.605>.
- 878 63. Sperry, J. S., Nichols, K. L., Sullivan, J. E., & Eastlack, S. E. (1994). Xylem  
879 embolism in ring-porous, diffuse-porous, and coniferous trees of northern  
880 Utah and interior Alaska. *Ecology*, 75(6), 1736-1752.  
881 <https://doi.org/10.2307/1939633>.
- 882 64. Thadani, R., Berlyn, G. P., & Ashton, M. S. (2009). A comparison of leaf  
883 physiology and anatomy of two Himalayan oaks in response to different light  
884 environments. *Journal of sustainable forestry*, 28(1-2), 74-91.  
885 <https://doi.org/10.1080/10549810802626159>.
- 886 65. Thompson, M. V. (2006). Phloem: the long and the short of it. *Trends in plant*  
887 *science*, 11(1), 26-32.
- 888 66. Tyree, M. T. (2003). Hydraulic limits on tree performance: transpiration,  
889 carbon gain and growth of trees. *Trees*, 17, 95-100.  
890 <https://doi.org/10.1007/s00468-002-0227-x>.
- 891 67. Tyree, M. T., & Sperry, J. S. (1989). Vulnerability of xylem to cavitation and  
892 embolism. *Annual review of plant biology*, 40(1), 19-36.  
893 <https://doi.org/10.1146/annurev.pp.40.060189.000315>.
- 894 68. Tyree, M.T., & Zimmermann, M.H. (2002). Hydraulic Architecture of Whole  
895 Plants and Plant Performance. In: *Xylem Structure and the Ascent of Sap*.  
896 Springer Series in Wood Science. Springer, Berlin, Heidelberg.  
897 [https://doi.org/10.1007/978-3-662-04931-0\\_6](https://doi.org/10.1007/978-3-662-04931-0_6)
- 898 69. Vaitkus, M. R., & McLeod, K. W. (1995). Photosynthesis and water-use  
899 efficiency of two sandhill oaks following additions of water and nutrients.  
900 *Bulletin of the Torrey Botanical Club*, 30-39.  
901 <https://doi.org/10.2307/2996401>.
- 902 70. Vignali, S., Barras, A. G., Arlettaz, R., & Braunisch, V. (2020). SDMtune: An  
903 R package to tune and evaluate species distribution models. *Ecology and*  
904 *Evolution*, 10(20), 11488-11506. <https://doi.org/10.1002/ece3.6786>.
- 905 71. Warton, D. I., Duursma, R. A., Falster, D. S., & Taskinen, S. (2012). smatr 3–  
906 an R package for estimation and inference about allometric lines. *Methods in*  
907 *ecology and evolution*, 3(2), 257-259. [https://doi.org/10.1111/j.2041-](https://doi.org/10.1111/j.2041-210X.2011.00153.x)  
908 [210X.2011.00153.x](https://doi.org/10.1111/j.2041-210X.2011.00153.x).

- 909 72. West, G. B., Brown, J. H., & Enquist, B. J. (1997). A general model for the  
910 origin of allometric scaling laws in biology. *Science*, 276(5309), 122-126.  
911 <https://doi.org/10.1126/science.276.5309.122>.
- 912 73. Will, T., & van Bel, A. J. (2006). Physical and chemical interactions between  
913 aphids and plants. *Journal of experimental botany*, 57(4), 729-737.  
914 <https://doi.org/10.1093/jxb/erj089>.
- 915 74. Will, T., Furch, A. C., & Zimmermann, M. R. (2013). How phloem-feeding  
916 insects face the challenge of phloem-located defenses. *Frontiers in plant  
917 science*, 4, 336.<https://doi.org/10.3389/fpls.2013.00336>.
- 918 75. Woodruff, D. R. (2014). The impacts of water stress on phloem transport in  
919 Douglas-fir trees. *Tree physiology*, 34(1), 5-14.  
920 <https://doi.org/10.1093/treephys/tpt106>.
- 921 76. Zanne, A.E., Tank, D.C., Cornwell, W.K., Eastman, J.M., Smith, S.A.,  
922 FitzJohn, R.G., McGlinn, D.J., O'Meara, B.C., Moles, A.T., Reich, P.B.,  
923 Royer, D.L., Soltis, D.E., Stevens, P.F., Westoby, M., Wright, I.J., Aarssen, L.,  
924 Bertin, R.I., Calaminus, A., Govaerts, R., Hemmings, F., Leishman, M.R.,  
925 Oleksyn, J., Soltis, P.S., Swenson, N.G., Warman, L., Beaulieu, J.M. (2014).  
926 Three keys to the radiation of angiosperms into freezing environments. *Nature*  
927 514, 394. <https://doi.org/10.1038/nature13842>.
- 928 77. Zhong, M., Cerabolini, B. E., Castro-Díez, P., Puyravaud, J. P., & Cornelissen,  
929 J. H. (2020). Allometric co-variation of xylem and stomata across diverse  
930 woody seedlings. *Plant, Cell & Environment*, 43(9), 2301-2310.  
931 <https://doi.org/10.1111/pce.13826>.
- 932 78. Zwieniecki, M. A., Melcher, P. J., Feild, T. S., & Holbrook, N. M. (2004). A  
933 potential role for xylem–phloem interactions in the hydraulic architecture of  
934 trees: effects of phloem girdling on xylem hydraulic conductance. *Tree  
935 Physiology*, 24(8), 911-917. <https://doi.org/10.1093/treephys/24.8.911>.

937 **TABLES**938 **Table 1.** Appendix of traits measured in this study; their abbreviations and units.

Parameter	Abbreviation	Unit
Leaf Area	<b>LA</b>	cm <sup>2</sup>
Petiole area	<b>A<sub>pet</sub></b>	μm <sup>2</sup>
Conductive area	<b>A<sub>c</sub></b>	μm <sup>2</sup>
Xylem area	<b>A<sub>x</sub></b>	μm <sup>2</sup>
Hydraulic diameter of xylem	<b>d<sub>hx</sub></b>	μm
Ratio xylem area/leaf area	<b>XLA</b>	cm <sup>2</sup> m <sup>-2</sup>
Hydraulic conductivity of xylem	<b>K<sub>hx</sub></b>	Kg m Mpa <sup>-1</sup> s <sup>-1</sup>
Specific conductivity of xylem	<b>K<sub>sx</sub></b>	Kg m <sup>-1</sup> Mpa <sup>-1</sup> s <sup>-1</sup>
Phloem area	<b>A<sub>p</sub></b>	μm <sup>2</sup>
Hydraulic diameter of phloem	<b>d<sub>hp</sub></b>	μm
Ratio phloem area/leaf area	<b>PLA</b>	cm <sup>2</sup> m <sup>-2</sup>
Hydraulic conductivity of phloem	<b>K<sub>hp</sub></b>	Kg m Mpa <sup>-1</sup> s <sup>-1</sup>
Photosynthesis net assimilation per leaf	<b>A<sub>N,leaf</sub></b>	μmol CO <sub>2</sub> s <sup>-1</sup>
Stomatal conductance per leaf	<b>g<sub>s,leaf</sub></b>	mmol H <sub>2</sub> O s <sup>-1</sup>
Mean annual temperature	<b>MAT</b>	°C
Mean annual precipitation	<b>MAP</b>	mm
Mean of daily minimum temperatures during the coldest quarter	<b>T<sub>min</sub></b>	°C
Aridity Index	<b>AI</b>	Dimensionless

939

940 **Table 2.** Percentage of variance explained by leaf habit (deciduous and evergreen)  
 941 according to the ANOVA performed for each trait measured individually. Leaf traits  
 942 notation as in Table 1. Significance level is showed with asterisks (\*\*\* < 0.001, \*\* =  
 943 0.001-0.01, \* = 0.01-0.05, n.s. > 0.05).

Trait	Leaf Habit	Residuals
<b>LA</b>	37.43 ***	62.57
<b>A<sub>pet</sub></b>	5.4 n.s.	94.6
<b>A<sub>c</sub></b>	14.12 *	85.88
<b>A<sub>x</sub></b>	13.97 ***	86.03
<b>d<sub>hx</sub></b>	32.51 ***	67.49
<b>XLA</b>	32.95 ***	67.05
<b>K<sub>hx</sub></b>	18.22 ***	81.78
<b>K<sub>sx</sub></b>	28.61 ***	71.39
<b>A<sub>p</sub></b>	11.72 ***	88.28

<b>d<sub>hp</sub></b>	25.17	***	74.83
<b>PLA</b>	29.23	***	70.77
<b>K<sub>hp</sub></b>	0.88	n.s.	99.12

944

945 **Table 3.** Scaling exponents of each leaf habit (deciduous and evergreen) separately for  
 946 standardized major axis (SMA) regressions. All variables were log<sub>10</sub> transformed. The  
 947 scaling relationship (isometry or allometry) was selected taking into account if the 95%  
 948 confident interval of the slope includes the value 1 (isometry) or not (allometry). All  
 949 correlations are significant ( $P < 0.001$ ) but  $K_{hp}$  with LA. Leaf traits notation as in Table  
 950 1. Differences in the slope and elevation between deciduous (DEC) and evergreen (EVE)  
 951 species are shown with asterisks ( $P < 0.001$  \*\*\*,  $P < 0.01$  \*\*,  $P < 0.05$  \*, NS = No  
 952 significant).

y	x	Figure	Deciduous			Evergreen			DEC vs EVE	
			Slope	Scaling relationship	R <sup>2</sup>	Slope	Scaling relationship	R <sup>2</sup>	Slope	Elevation
A <sub>pet</sub>	LA	Fig. 4a	0.73	Allometry	0.486	0.9	Isometry	0.752	*	***
A <sub>c</sub>	LA	Fig. 4b	0.71	Allometry	0.816	0.79	Allometry	0.816	NS	***
A <sub>x</sub>	LA	Fig. 5a	0.74	Allometry	0.874	0.76	Allometry	0.651	NS	***
d <sub>hx</sub>	LA	Fig. 5b	0.33	Allometry	0.507	0.37	Allometry	0.563	NS	NS
XLA	LA	Fig. 5c	-0.4	Allometry	0.579	-0.59	Allometry	0.429	*	*
A <sub>p</sub>	LA	Fig. 5d	0.75	Allometry	0.599	0.87	Allometry	0.69	NS	***
d <sub>hp</sub>	LA	Fig. 5e	0.24	Allometry	0.2	0.24	Allometry	0.443	NS	*
PLA	LA	Fig. 5f	-0.63	Allometry	0.439	-0.56	Allometry	0.24	NS	NS
A <sub>p</sub>	A <sub>x</sub>	Fig. 51	1.01	Isometry	0.716	1.15	Allometry	0.811	NS	NS
K <sub>hx</sub>	LA	Fig. 6a	1.57	Allometry	0.724	1.66	Allometry	0.56	NS	NS
K <sub>sx</sub>	LA	Fig. 6b	1	Isometry	0.415	1.18	Isometry	0.281	NS	NS
K <sub>hp</sub>	LA	Plot not shown	1.13	Isometry	0.276	1.61	Isometry	0.036	NS	NS

953

954 **Table 4.** Scaling exponents of physiological traits for standardized major axis (SMA)  
 955 regressions. All variables were log<sub>10</sub> transformed. Leaf traits notation as in Table 1. Every  
 956 correlation is significant ( $P < 0.05$ ) and scale allometrically (slope significantly different  
 957 of 1).

y	x	Figure	Slope	Scaling relationship	R <sup>2</sup>
A <sub>x</sub>	<b>g<sub>s,leaf</sub></b>	Fig. 8a	0.61	Allometry	0.512
d <sub>hx</sub>	<b>g<sub>s,leaf</sub></b>	Fig. 8b	0.38	Allometry	0.586
K <sub>hx</sub>	<b>g<sub>s,leaf</sub></b>	Fig. 8c	1.86	Allometry	0.684
A <sub>x</sub>	<b>A<sub>N,leaf</sub></b>	Fig. 8d	0.63	Allometry	0.591
d <sub>hx</sub>	<b>A<sub>N,leaf</sub></b>	Fig. 8e	0.39	Allometry	0.671
K <sub>hx</sub>	<b>A<sub>N,leaf</sub></b>	Fig. 8f	1.91	Allometry	0.786
A <sub>p</sub>	<b>A<sub>N,leaf</sub></b>	Fig. 9a	0.73	Allometry	0.561
d <sub>hp</sub>	<b>A<sub>N,leaf</sub></b>	Fig. 9b	0.23	Allometry	0.509

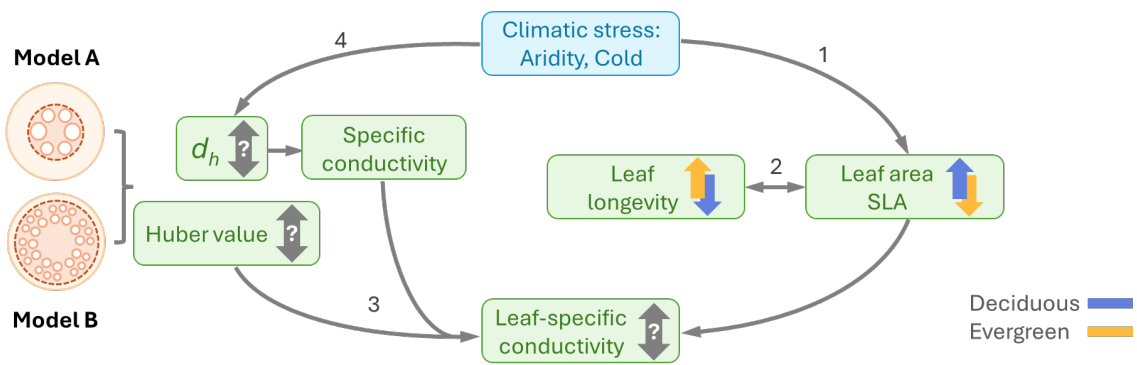
958



959 **Table 5.** References of studies exploring the scaling relationship between xylem and  
960 phloem conductive areas, specifying the species and organs studied as well as the slope  
961 and the nature of the scaling found, either isometry or allometry.

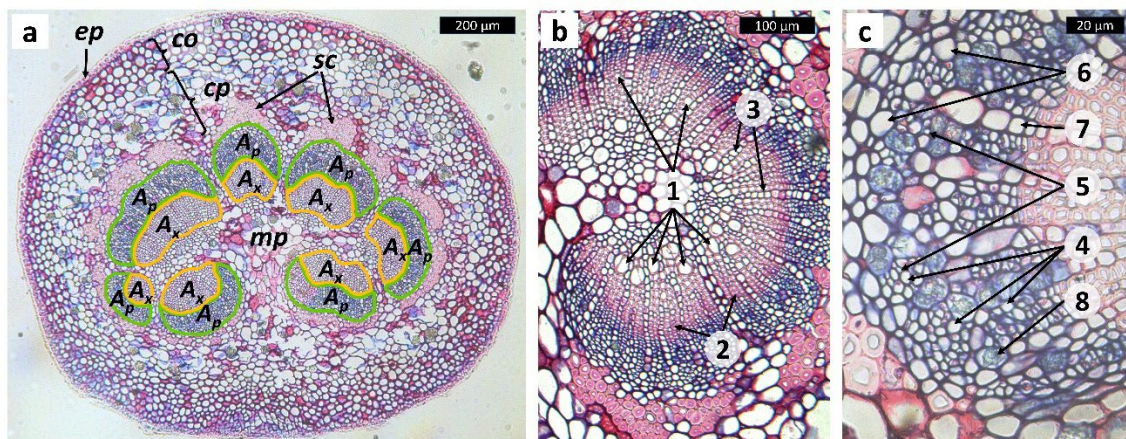
Reference	Species	Organ	Slope	Scaling relationship
Jyske and Hölttä 2015	<i>Picea abies</i>	Stem	0.93	Isometry
Carvalho et al. 2017a	<i>Populus × canescens</i>	Leaf, petiole	0.96	Isometry
Carvalho et al. 2017b	<i>Ginkgo biloba</i>	Leaf	0.91	Isometry
Kiorapostolou and Petit 2019	<i>Fraxinus ornus</i>	Stem	0.96	Isometry
962 Ray and Jones 2018	<i>Pelargonium</i> (11 spp.)	Petiole	0.87	Isometry

963



965

966 **Fig. 1.** Scheme of the traits that ultimately modulate the leaf-specific conductivity (LSC)  
 967 of the petiole. Thick colored arrows show the tendency of each leaf habit (deciduous in  
 968 blue and evergreen in orange) to have larger (upward arrow) or smaller (downward arrow)  
 969 values for leaf longevity, leaf area and specific leaf area (SLA). Thick grey arrows  
 970 represent the unknown relationships we aim to explore in this study. Two anatomical  
 971 models are proposed: model A assumes that LSC can be improved increasing the  
 972 hydraulic diameter ( $d_h$ ), whereas model B assumes that for the same cross-section of  
 973 petiole, a similar LSC could be reached by increasing the conductive area with a smaller  
 974  $d_h$ . References that support the proposed relationships are: 1) Sancho-Knapik et al.  
 975 (2021); 2) Mediavilla et al. (2008) and Kikuzawa et al. (2013); 3) Mencuccini et al.  
 976 (2019). 4) Blackman et al. (2023).

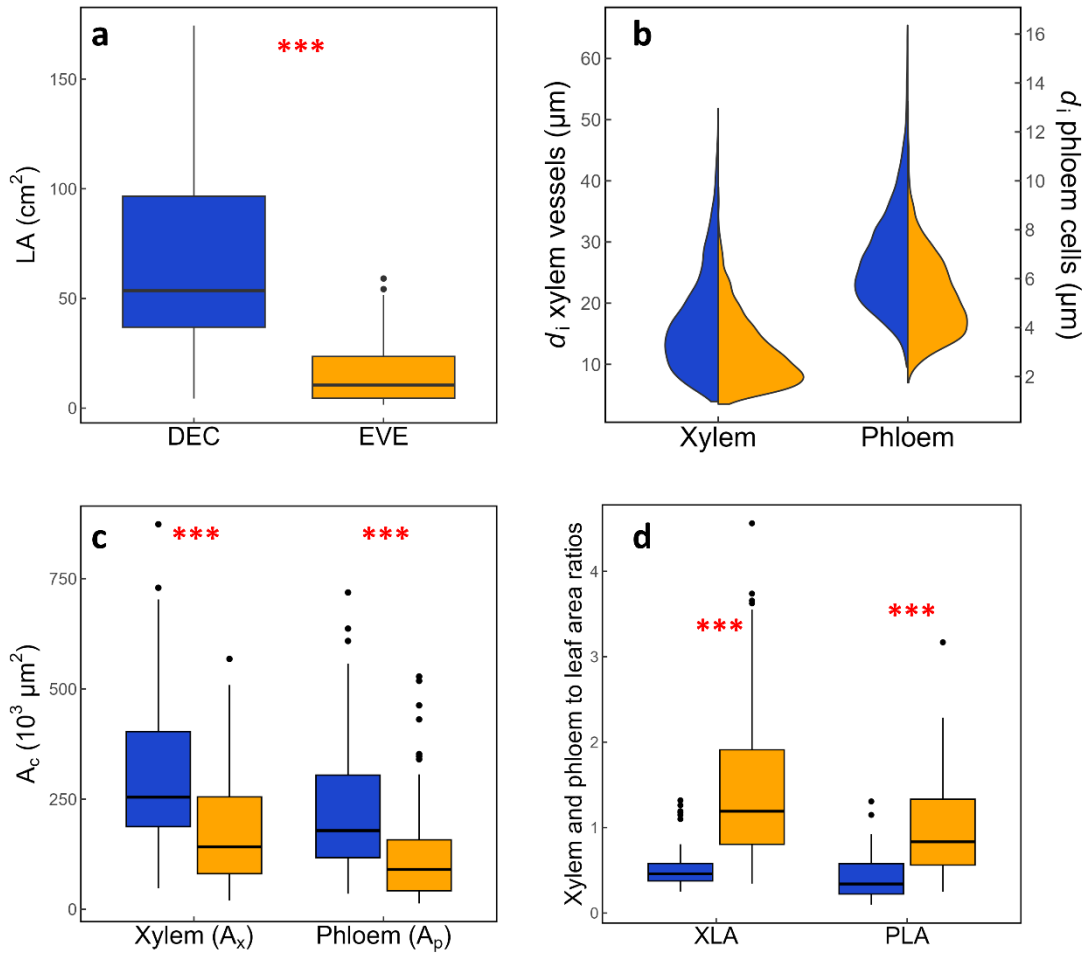


977

978 **Fig. 2.** Histological cross-section of *Quercus agrifolia* petiole. **(a) General scheme** of the  
 979 whole petiole with the main tissues: epidermis (ep), collenchyma (co), cortical  
 980 parenchyma (cp), sclerenchyma (sc), medullary parenchyma (mp) and the conductive  
 981 tissues, measured in this study: xylem ( $A_x$ , highlighted in yellow) and phloem ( $A_p$ ,  
 982 highlighted in green). **(b) Magnified view of xylem** with its main cellular types: xylem

983 vessels (1; measured in this study), tracheids (2) and parenchymatic medullary rays (3).  
984 **(c) Detailed view of phloem** with its main cellular types: potential sieve tubes (4;  
985 measured in this study), potential companion cells (5), phloem fibers (6), medullary rays  
986 (7) and parenchyma (8).

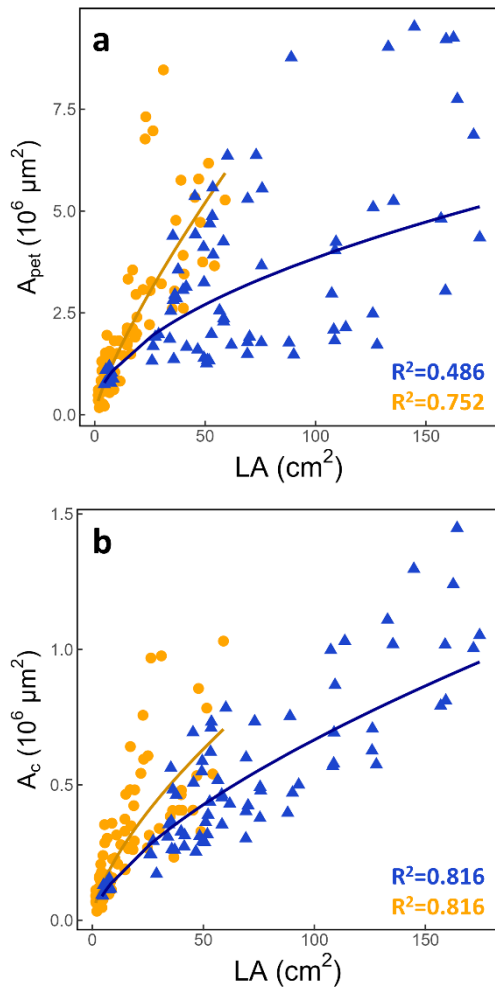
987



988

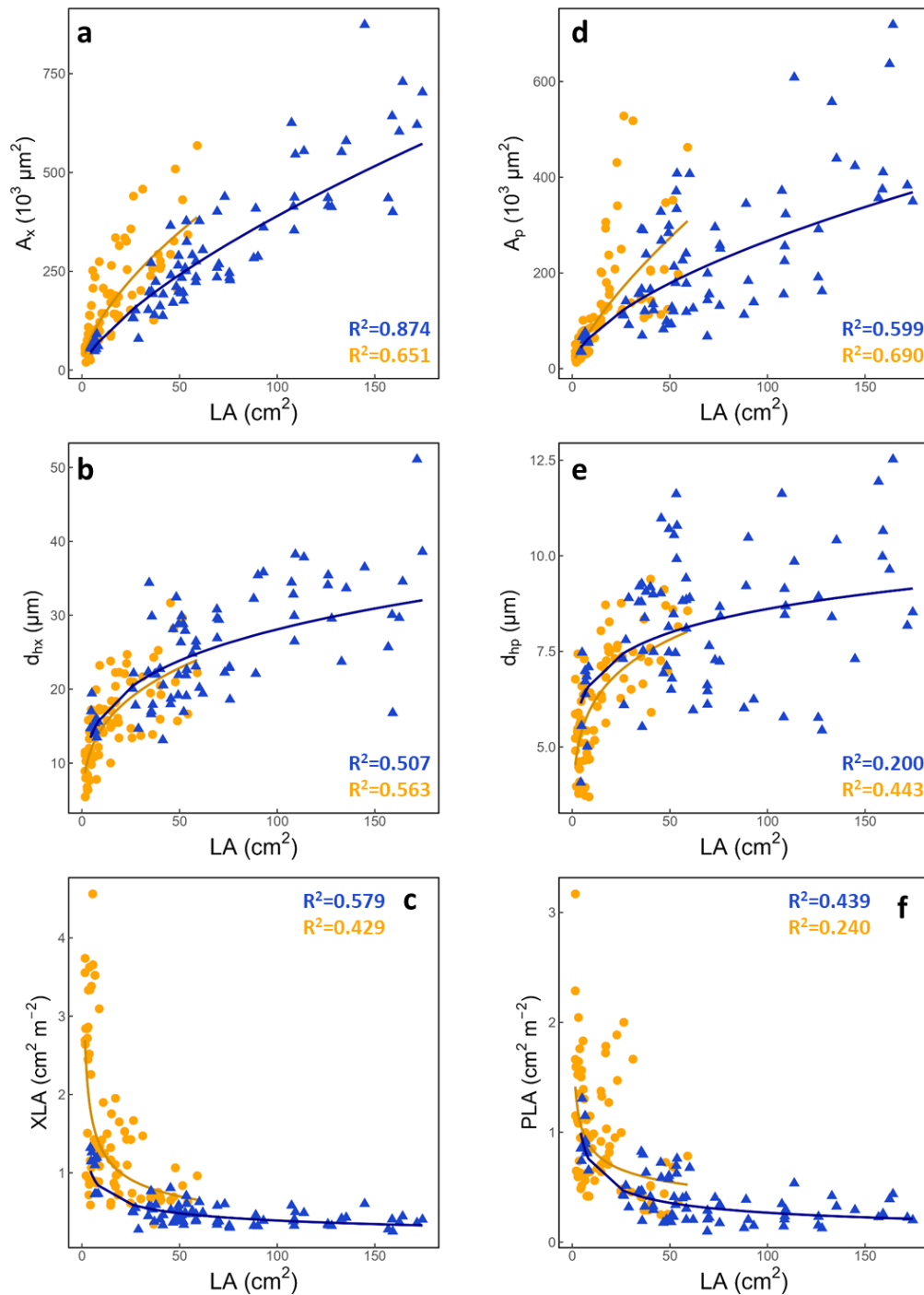
989 **Fig. 3.** Distribution of the main traits measured: a) Boxplot of the leaf area (LA), b) Violin  
 990 plot of the diameters ( $d_i$ ) of the conduits (vessels for xylem and sieve tubes for phloem),  
 991 c) Boxplot total conductive area ( $A_c$ ) in the petiole, and d) Xylem and phloem to leaf area  
 992 ratios, i.e., conductive area divided by LA. Red asterisks show significant ( $P < 0.001$ )  
 993 differences between leaf habits (blue, deciduous; orange, evergreen). Note the double Y  
 994 scale in panel b).

995



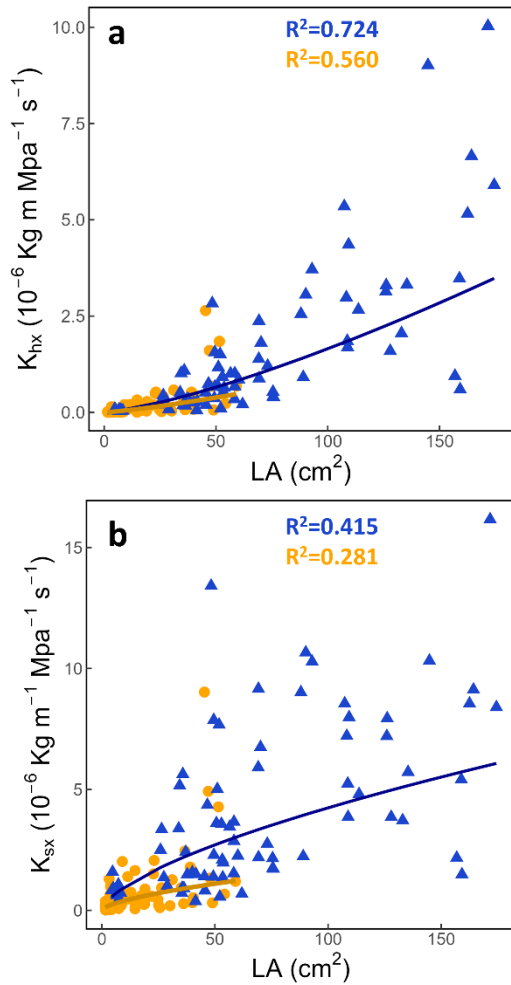
996

997 **Fig. 4.** Scaling relationships of a) leaf area (LA) with cross-sectional petiole area ( $A_{pet}$ )  
 998 and b) LA with conductive area ( $A_c$ , the sum of xylem and phloem areas) for deciduous  
 999 (blue triangles) and evergreen (orange dots) species. Each point represents one individual  
 1000 measure. Colored continuous lines represent the best fit for each leaf habit separately. All  
 1001 regressions are highly significant ( $P < 0.001$ ).



1002

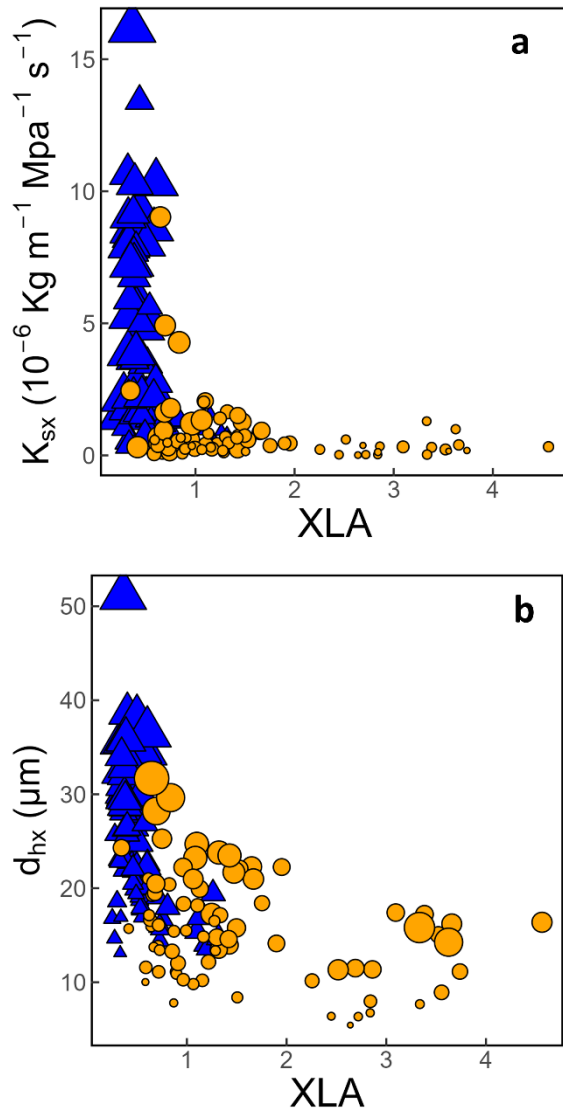
1003 **Fig. 5.** Correlations related to xylem (panels a-c) and phloem (panels d-f) anatomy for  
 1004 deciduous (blue triangles) and evergreen (orange dots) species between leaf area (LA)  
 1005 and: a) xylem cross-sectional area ( $A_x$ ), b) xylem hydraulic diameter ( $d_{hx}$ ), c) xylem cross-  
 1006 sectional area divided by LA (XLA), d) phloem cross-sectional area ( $A_p$ ), e) phloem  
 1007 hydraulic diameter ( $d_{hp}$ ) and f) phloem cross-sectional area divided by LA (PLA). Each  
 1008 point represents one individual measure. Colored continuous lines represent the best fit  
 1009 for each leaf habit separately. All regressions are highly significant ( $P < 0.001$ ).



1010

1011 **Fig. 6.** Correlations related to a) xylem hydraulic conductivity ( $K_{hx}$ ) and b) specific  
 1012 hydraulic conductivity ( $K_{sx}$ ) for deciduous (blue triangles) and evergreen (orange dots)  
 1013 species. Each point represents one individual measure. Colored continuous lines represent  
 1014 the best fit for each leaf habit separately. All regressions are highly significant ( $P < 0.001$ ).

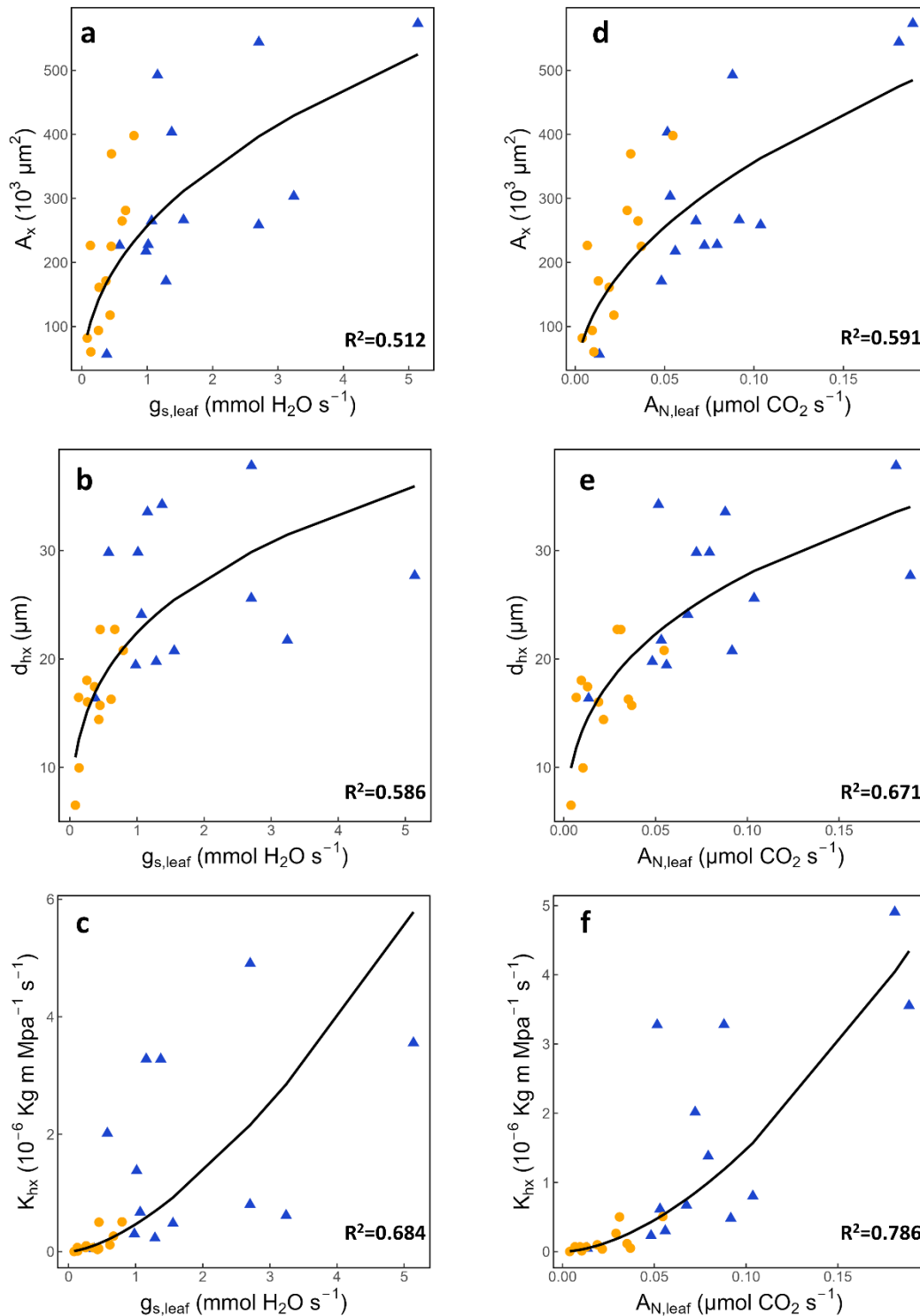
1015



1016

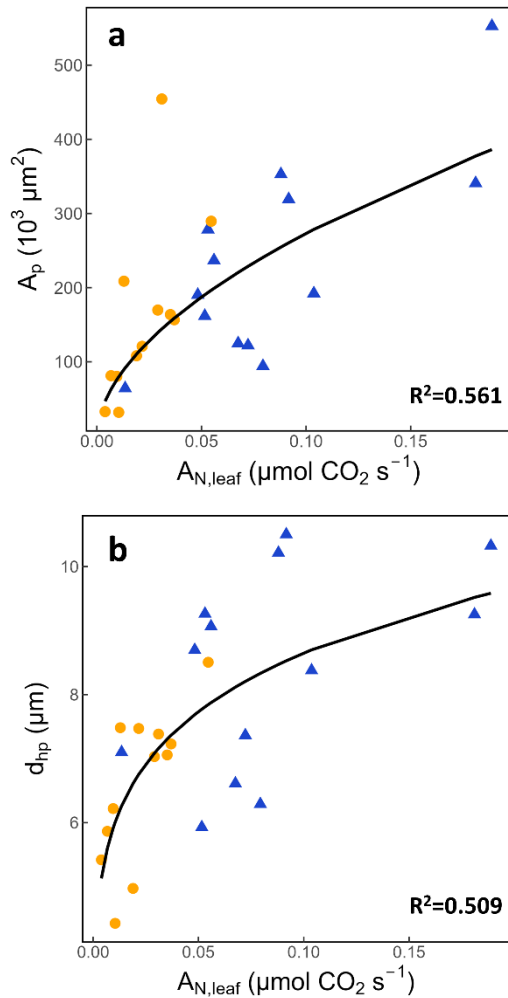
1017 **Fig. 7.** Correlations between a) XLA and the xylem specific conductivity ( $K_{sx}$ ) showing  
 1018 the leaf area as the relative size of the symbols (larger symbols represent larger leaf areas);  
 1019 and b) between the XLA and the xylem hydraulic diameter ( $d_{hx}$ ) showing the leaf specific  
 1020 conductivity (LSC) as the relative size of the symbols (larger symbols show higher LSC  
 1021 values). Leaf habit is represented by deciduous in blue triangles and evergreen species in  
 1022 orange dots. Each point represents one individual measure.





1023

1024 **Fig. 8.** Relationships between xylem traits (cross-sectional area ( $A_x$ ), hydraulic diameter  
 1025 ( $d_{hx}$ ) and calculated hydraulic conductivity ( $K_{hx}$ ), stomatal conductance ( $g_{s,leaf}$ ) and  
 1026 photosynthesis net rate ( $A_{N,leaf}$ ). Blue triangles are deciduous and orange dots are  
 1027 evergreen species. Each point represents the mean value of a species. The black  
 1028 continuous line is the correlation considering species altogether. All regressions are highly  
 1029 significant ( $P < 0.001$ ).



1031

1032 **Fig. 9.** Main relationships between photosynthesis net rate ( $A_{N,leaf}$ ) and phloem anatomical  
 1033 traits (cross-sectional area ( $A_p$ ) and hydraulic diameter ( $d_{hp}$ )). Deciduous as blue triangles  
 1034 and evergreen species as orange dots. Each point represents the mean value of a species.  
 1035 The black continuous line is the correlation considering species altogether. Both  
 1036 regressions are highly significant ( $P < 0.001$ ).